# Chapter 6

# Spherical Waves

## 6.1 Introduction

Wave expansions in cylindrical and planar geometries consist of wavefronts which extend to infinity in at least one dimension. The spherical geometry provides a finite and compact expansion of wavefronts which allows us to gain an understanding of expanding waves. Furthermore, compact, realistic vibrators are more closely modeled with spherical wave expansions than with planar or cylindrical expansions. We present in this chapter the solution of the wave equation in spherical coordinates, and detailed discussions of the radial functions, spherical harmonics and multipole expansions, the latter being very useful for low frequency modeling of radiation from compact vibrators.

The spherical wave spectrum, analog of the helical wave spectrum, is introduced to follow the formulations for plane and cylindrical geometries with regard to the forward and backward propagation of spherical waves for both internal and external problems. Various radiation problems are solved.

## 6.2 The Wave Equation

The coordinate system is given in Fig. 6.1 and is related to rectangular coordinates through

$$\begin{aligned} x &= r\sin\theta\cos\phi, \\ y &= r\sin\theta\sin\phi, \\ z &= r\cos\theta. \end{aligned} \tag{6.1}$$

so that $r = \sqrt{x^2+y^2+z^2}$, $\theta = \tan^{-1}[\sqrt{x^2+y^2}/z]$, and $\phi = \tan^{-1}[y/x]$.

The time dependent wave equation given in spherical coordinates is

$$\frac{1}{r^2}\frac{\partial}{\partial r}(r^2\frac{\partial p}{\partial r}) + \frac{1}{r^2\sin\theta}\frac{\partial}{\partial\theta}(\sin\theta\frac{\partial p}{\partial\theta}) + \frac{1}{r^2\sin^2\theta}\frac{\partial^2 p}{\partial\phi^2} - \frac{1}{c^2}\frac{\partial^2 p}{\partial t^2} = 0. \tag{6.2}$$

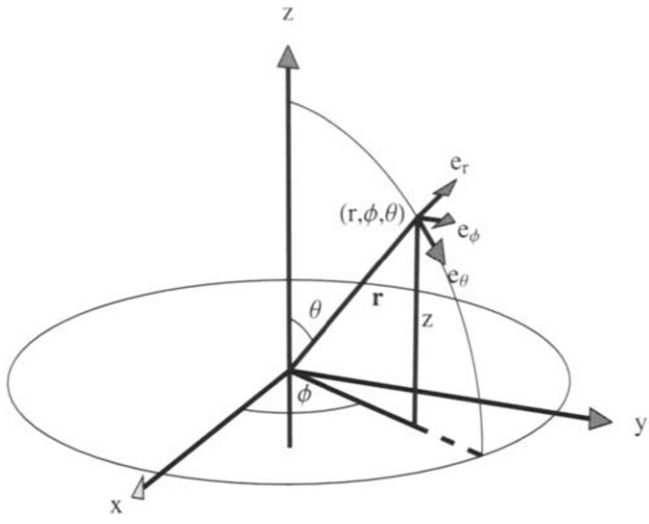


**Figure 6.1:** Definition of spherical coordinates relative to Cartesian coordinates. $\phi$ is measured in the $x, y$ plane from the $x$ axis (azimuthal direction). $\theta$ is measured from the polar axis, $z$.

It is useful to note that

$$\frac{1}{r^2}\frac{\partial}{\partial r}(r^2\frac{\partial p}{\partial r}) = \frac{1}{r}\frac{\partial^2}{\partial r^2}(rp). \tag{6.3}$$

The gradient of the pressure given in spherical coordinates is

$$\vec{\nabla}p = \hat{e}_r\frac{\partial p}{\partial r} + \hat{e}_\theta\frac{1}{r}\frac{\partial p}{\partial \theta} + \hat{e}_o\frac{1}{r\sin\theta}\frac{\partial p}{\partial \phi}, \tag{6.4}$$

where $(\hat{e}_r, \hat{e}_\theta, \hat{e}_\phi)$ represent unit vectors in each of the coordinate directions as shown in Fig. 6.1. Euler's equation is given by (Eq. (2.14), page 19)

$$i\rho_0 ck\vec{v}(r,\theta,\phi) = \vec{\nabla}p(r,\theta,\phi), \tag{6.5}$$

where

$$\vec{v} \equiv \dot{u}\hat{e}_\theta + \dot{v}\hat{e}_o + \dot{w}\hat{e}_r. \tag{6.6}$$

The solution of Eq. (6.2) is given by separation of variables:

$$p(r,\theta,\phi,t) = R(r)\Theta(\theta)\Phi(\phi)T(t), \tag{6.7}$$

which leads to four ordinary differential equations:[1]

$$\frac{d^2\Phi}{d\phi^2} + m^2\Phi = 0, \tag{6.8}$$

$$\frac{1}{\sin\theta}\frac{d}{d\theta}(\sin\theta\frac{d\Theta}{d\theta}) + [n(n+1) - \frac{m^2}{\sin^2\theta}]\Theta = 0, \tag{6.9}$$

$$\frac{1}{r^2}\frac{d}{dr}(r^2\frac{dR}{dr}) + k^2R - \frac{n(n+1)}{r^2}R = 0, \tag{6.10}$$

$$\frac{1}{c^2}\frac{d^2T}{dt^2} + k^2T = 0. \tag{6.11}$$

The solution to Eq. (6.11) is, with $k = \omega/c$,

$$T(\omega) = T_1e^{i\omega t} + T_2e^{-i\omega t}. \tag{6.12}$$

and again we choose the second solution for our time dependence, so that $T_1 = 0$.

The solution to Eq. (6.8) is

$$\Phi(\phi) = \Phi_1e^{im\phi} + \Phi_2e^{-im\phi}. \tag{6.13}$$

or, alternatively,

$$\Phi(\phi) = \Phi_3\cos(m\phi) + \Phi_4\sin(m\phi). \tag{6.14}$$

We keep both solutions in these cases. In both these cases $m$ must be an integer so that there is continuity and periodicity of $\Phi(\phi)$.

The orthogonality relation for the azimuthal functions is

$$\int_0^{2\pi} e^{-im'\phi}e^{im\phi}d\phi = 2\pi\delta_{mm'}. \tag{6.15}$$

The solution to Eq. (6.9) is found using a transformation of variables. Let $\eta = \cos\theta$ $(-1 \le \eta \le 1)$ so that the differential equation for $\Theta$ becomes

$$\frac{d}{d\eta}[(1-\eta^2)\frac{d\Theta}{d\eta}] + [n(n+1) - \frac{m^2}{1-\eta^2}]\Theta = 0. \tag{6.16}$$

The solutions are given by Legendre functions of the first and second kinds,

$$\Theta(\theta) = \Theta_1P_n^m(\cos\theta) + \Theta_2Q_n^m(\cos\theta). \tag{6.17}$$

The functions of the second kind, $Q_n^m$ are not finite at the poles where $\eta = \pm 1$ so this solution is discarded ($\Theta_2 = 0$). The functions of the first kind diverge at $\cos\theta = 1$ ($\theta = 0$) unless we restrict $n$ to be an integer. Furthermore, when $n$ is an integer then $P_n^m(\eta) = 0$ when $m > n$. We will discuss the functions of the first kind in more detail later.

Finally for the radial differential equation, Eq. (6.10), the solutions are

$$R(r) = R_1j_n(kr) + R_2y_n(kr). \tag{6.18}$$

[1]E. Skudrzyk (1971). *Foundations of Acoustics*. Springer-Verlag, New York, pp. 379–380.

where $j_n$ and $y_n$ are spherical Bessel functions of the first and second kind, respectively. Alternatively, the solutions can be written as

$$R(r) = R_3 h_n^{(1)}(kr) + R_4 h_n^{(2)}(kr), \tag{6.19}$$

where $h_n^{(1)}$ and $h_n^{(2)}$ are spherical Hankel functions. Just as with the cylindrical Bessel functions it is true that

$$h_n^{(1)}(kr) \propto e^{ikr},$$

representing an outgoing wave and

$$h_n^{(2)}(kr) \propto e^{-ikr},$$

representing an incoming wave. We may keep one or both of these solutions depending upon the locations of the sources in the problem.

The angle functions are conveniently combined into a single function called a spherical harmonic $Y_n^m$ defined by

$$Y_n^m(\theta, \phi) \equiv \sqrt{\frac{(2n+1)}{4\pi}\frac{(n-m)!}{(n+m)!}} P_n^m(\cos\theta) e^{im\phi}. \tag{6.20}$$

We will study spherical harmonics in detail in Section 6.3.3.

We can write any solution to Eq. (6.2), with $e^{-i\omega t}$ implicit, as

$$p(r, \theta, \phi, \omega) = \sum_{n=0}^{\infty} \sum_{m=-n}^{n} \left(A_{mn} j_n(kr) + B_{mn} y_n(kr)\right) Y_n^m(\theta, \phi) \tag{6.21}$$

for standing wave type solutions and

$$p(r, \theta, \phi, \omega) = \sum_{n=0}^{\infty} \sum_{m=-n}^{n} \left(C_{mn} h_n^{(1)}(kr) + D_{mn} h_n^{(2)}(kr)\right) Y_n^m(\theta, \phi) \tag{6.22}$$

for traveling wave solutions. We now study the properties of these function in more detail.

## 6.3 The Angle Functions

### 6.3.1 Legendre Polynomials

Solutions of Eq. (6.16) in which $m = 0$ are very important. These represent fields which have no variation in the azimuthal direction $\phi$. The convention is to define

$$P_n^0(x) \equiv P_n(x).$$

These functions are polynomials of degree $n$. The general form is

$$\begin{aligned} P_n(x) &= \frac{(2n-1)!!}{n!}\Big[x^n - \frac{n(n-1)}{2\cdot(2n-1)}x^{n-2} \\ &+ \frac{n(n-1)(n-2)(n-3)}{2\cdot 4\cdot(2n-1)(2n-3)}x^{n-4} \\ &- \frac{n(n-1)(n-2)(n-3)(n-4)(n-5)}{2\cdot 4\cdot 6\cdot(2n-1)(2n-3)(2n-5)}x^{n-6} + \cdots\Big], \quad n = 0, 1, 2, \cdots. \end{aligned} \tag{6.23}$$

(The last term in square brackets occurs when the exponent of $x$ is zero or one.) Also, $(2n-1)!! \equiv (2n-1)(2n-3)\cdots 1$. It is clear from Eq. (6.23) that Legendre polynomials obey

$$P_n(-x) = (-1)^n P_n(x). \tag{6.24}$$

The Legendre polynomials take on the following special values:

$$\begin{aligned} P_n(1) &= 1 \\ P_n(-1) &= (-1)^n \\ P_n(0) &= (-1)^{n/2}\frac{1\cdot 3\cdot 5\cdots(n-1)}{2\cdot 4\cdot 6\cdots n}, \quad n \text{ even} \\ &= 0 \qquad\qquad n \text{ odd.} \end{aligned} \tag{6.25}$$

The first six Legendre polynomials are

| | |
|---|---|
| $P_0(x) = 1$ | $P_3(x) = \frac{1}{2}(5x^3 - 3x)$ |
| $P_1(x) = x$ | $P_4(x) = \frac{1}{8}(35x^4 - 30x^2 + 3)$ |
| $P_2(x) = \frac{1}{2}(3x^2 - 1)$ | $P_5(x) = \frac{1}{8}(63x^5 - 70x^3 + 15x).$ |

(6.26)

These are plotted in Fig. 6.2 as a function of $\theta$, where $x = \cos\theta$.

Equation (6.23) can be written in more concise form called Rodrigues' Formula:

$$P_n(x) = \frac{1}{2^n n!}\frac{d^n}{dx^n}(x^2-1)^n. \tag{6.27}$$

The Legendre polynomials are orthogonal and

$$\int_{-1}^{1} P_n(x)P_m(x)dx = \frac{2}{2n+1}\delta_{nm}. \tag{6.28}$$

### 6.3.2 Associated Legendre Functions

The associated Legendre functions are given by two integer indices $P_n^m(x)$. For positive $m$ these are related to the Legendre polynomials by the formula,[2]

$$P_n^m(x) = (-1)^m(1-x^2)^{m/2}\frac{d^m}{dx^m}P_n(x). \tag{6.29}$$

The series representation is[3]

$$\begin{aligned} P_n^m(x) &= \frac{(-1)^m(2n-1)!!}{(n-m)!}(1-x^2)^{m/2}\Big[x^{n-m} - \frac{(n-m)(n-m-1)}{2(2n-1)}x^{n-m-2} \\ &+ \frac{(n-m)(n-m-1)(n-m-2)(n-m-3)}{2\cdot 4(2n-1)(2n-3)}x^{n-m-4} - \cdots\Big], \end{aligned} \tag{6.30}$$

[2] I. S. Gradshteyn and I. M. Ryzhik (1965). *Table of Integrals, Series and Products.* 4th ed., Academic Press, N.Y.

[3] Gradshteyn and Ryzhik, *Table of Integrals, Series and Products.*

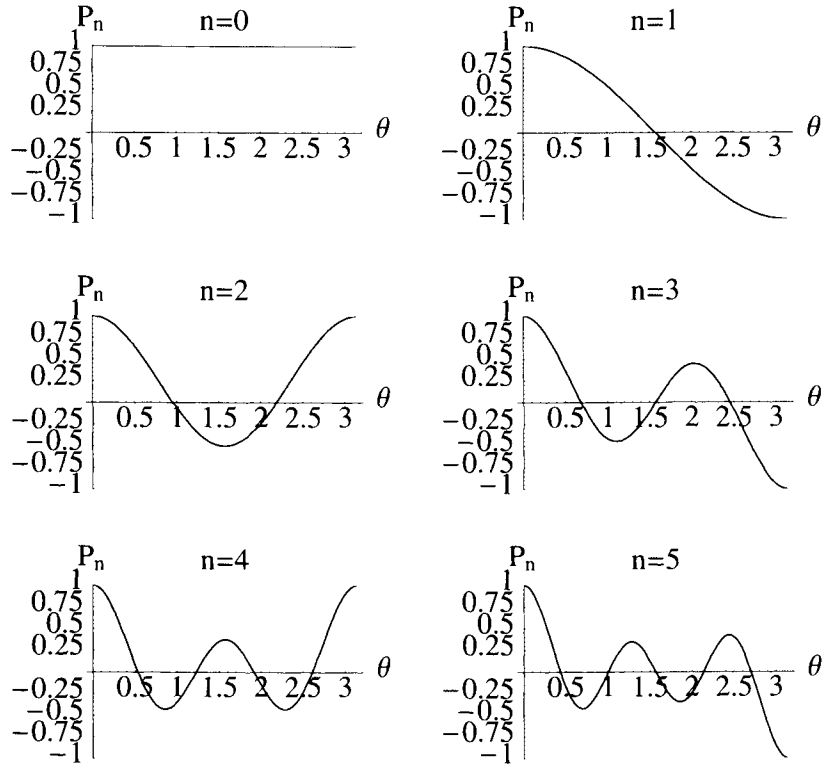


**Figure 6.2:** Plots of the Legendre polynomials, $P_n(\cos\theta)$, as a function of $\theta$ for $n = 0, 1, 2, 3, 4, 5$.

where the series truncates when the numerator goes to zero.

Note that sometimes in the literature the associated Legendre functions are defined differently, without the $(-1)^m$ after the equal sign in Eq. (6.29). Equation (6.29) can not be used to generate the functions for $m < 0$. In this case the associated Legendre function is defined as

$$P_n^{-m}(x) \equiv (-1)^m \frac{(n-m)!}{(n+m)!} P_n^m(x) \tag{6.31}$$

where $m$ is positive.

For each $m$ the functions $P_n^m(x)$ form a complete set of orthogonal functions which obey the relation:

$$\int_{-1}^{1} P_{n'}^m(x) P_n^m(x)\, dx = \frac{2}{2n+1} \frac{(n+m)!}{(n-m)!} \delta_{n'n}. \tag{6.32}$$

The orthogonality integral for the $m = 0$ case was already given in Eq. (6.28).

Following is a partial list of associated Legendre functions, grouped by orthogonal

sets:

| $m = 0$ | $m = 1$ |
|---|---|
| $P_0^0 = 1$ | $P_1^1 = -\sin\theta$ |
| $P_1^0 = \cos\theta$ | $P_2^1 = -3\cos\theta\sin\theta$ |
| $P_2^0 = \dfrac{1+3\cos 2\theta}{4}$ | $P_3^1 = \dfrac{3\left(1-5\cos^2\theta\right)\sin\theta}{2}$ |
| $P_3^0 = \dfrac{-3\cos\theta+5\cos^3\theta}{2}$ | $P_4^1 = \dfrac{5\left(3\cos\theta-7\cos^3\theta\right)\sin\theta}{2}$ |

(6.33)

| $m = 2$ | $m = 3$ & $4$ |
|---|---|
| $P_2^2 = 3\sin^2\theta$ | $P_3^3 = -15\sin^3\theta$ |
| $P_3^2 = 15\cos\theta\sin^2\theta$ | $P_4^3 = -105\cos\theta\sin^3\theta$ |
| $P_4^2 = \dfrac{15\,(5+7\cos 2\theta)\sin^2\theta}{4}$ | $P_4^4 = 105\sin^4\theta$ |

(6.34)

Due to the definition, Eq. (6.31), the functions for negative $m$ differ only by a constant from the corresponding functions for positive $m$:

| $m = -1$ | $m = -2$ |
|---|---|
| $P_1^{-1} = \dfrac{\sin\theta}{2}$ | $P_2^{-2} = \dfrac{\sin^2\theta}{8}$ |
| $P_2^{-1} = \dfrac{\cos\theta\sin\theta}{2}$ | $P_3^{-2} = \dfrac{\cos\theta\sin^2\theta}{8}$ |
| $P_3^{-1} = \dfrac{(3+5\cos 2\theta)\sin\theta}{16}$ | $P_4^{-2} = \dfrac{(5+7\cos 2\theta)\sin^2\theta}{96}$ |

(6.35)

Figure 6.3 shows an example of associated Legendre functions. The first six of the functions for $m = 1$ are plotted. Note that they are orthogonal, satisfying Eq. (6.32).

The associated Legendre functions for $m = 3$ are plotted in Fig. 6.4 for comparison with Fig. 6.3. The first six orthogonal functions ($n = 3 - 8$) are shown. Note that as $m$ increases the functions are more tapered at the two poles. The increase in the number of oscillations is linearly proportional to the increase in $m$.

The recurrence relations for the Legendre functions can be written in numerous ways.[4] Four derivative relations are

$$(1-x^2)\frac{dP_n^m(x)}{dx} = (n+1)xP_n^m(x) - (n-m+1)P_{n+1}^m(x)r, \tag{6.36}$$

$$= -nxP_n^m(x) + (n+m)P_{n-1}^m(x), \tag{6.37}$$

$$= -\sqrt{1-x^2}P_n^{m+1}(x) - mxP_n^m(x), \tag{6.38}$$

$$= (n-m+1)(n+m)\sqrt{1-x^2}P_n^{m-1}(x) + mxP_n^m(x). \tag{6.39}$$

[4]Gradshteyn and Ryzhik, *Table of Integrals, Series and Products*, p.1005.

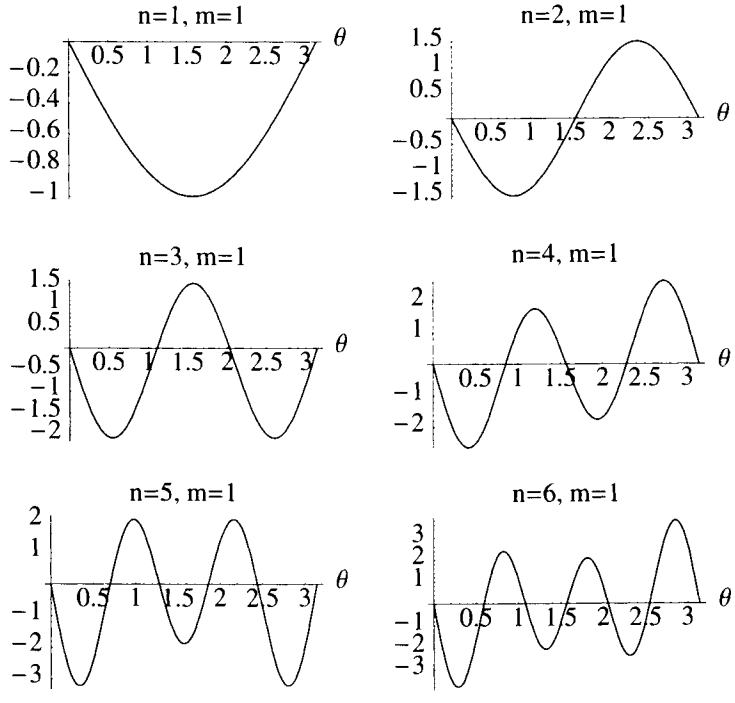


**Figure 6.3:** Plots of the associated Legendre functions, $P_n^m(\cos\theta)$, as a function of $\theta$ for $n = 1, 2, 3, 4, 5, 6$ and $m = 1$.

Four recurrence relations not involving derivatives are

$$(2n+1)xP_n^m(x) = (n-m+1)P_{n+1}^m(x) + (n+m)P_{n-1}^m(x), \tag{6.40}$$

$$P_n^{m+2}(x) = -2(m+1)\frac{x}{\sqrt{1-x^2}}P_n^{m+1}(x) - (n-m)(n+m+1)P_n^m(x), \tag{6.41}$$

$$P_{n-1}^m(x) - P_{n+1}^m(x) = (2n+1)\sqrt{1-x^2}P_n^{m-1}(x), \tag{6.42}$$

$$P_{-n-1}^m(x) = P_n^m(x). \tag{6.43}$$

Many other recurrence relations can be developed from these. In the appropriate relations above, putting $m = 0$ generates the recurrence relationships for the Legendre polynomials.

### 6.3.3 Spherical Harmonics

Equation 6.20 above defined the spherical harmonics as

$$Y_n^m(\theta,\phi) \equiv \sqrt{\frac{(2n+1)}{4\pi}\frac{(n-m)!}{(n+m)!}}P_n^m(\cos\theta)e^{im\phi}.$$

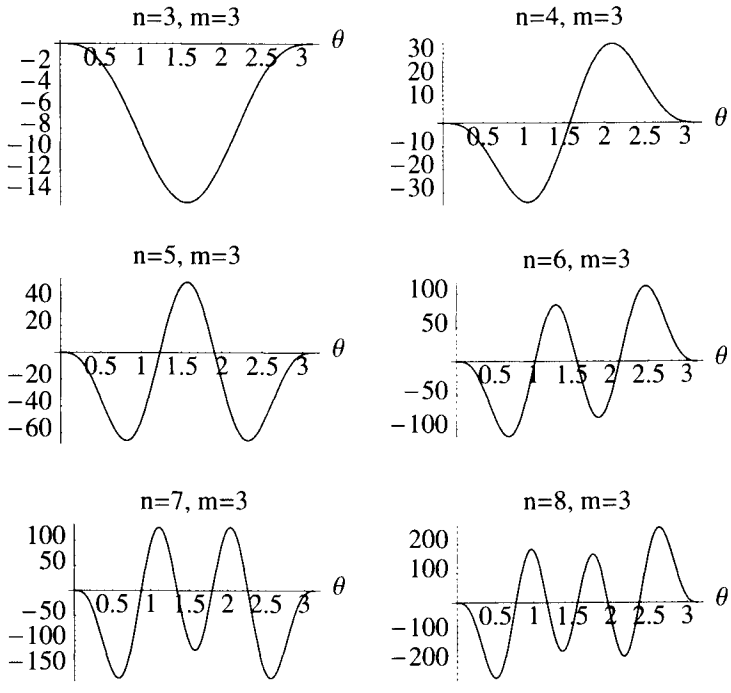


**Figure 6.4:** Plots of the associated Legendre functions $P_n^m(\cos\theta)$ as a function of $\theta$ for $n = 3, 4, 5, 6, 7, 8$ and $m = 3$.

Due to Eq. (6.31) we have

$$Y_n^{-m}(\theta, \phi) = (-1)^m Y_n^m(\theta, \phi)^*. \tag{6.44}$$

The spherical harmonics $Y_n^m$ are orthonormal:

$$\int_0^{2\pi} d\phi \int_0^{\pi} Y_n^m(\theta, \phi) Y_{n'}^{m'}(\theta, \phi)^* \sin\theta d\theta = \delta_{nn'}\delta_{mm'}. \tag{6.45}$$

Earlier we learned that for any complete set of orthonormal functions $U_n(\zeta)$ there exists a completeness or closure relation given by

$$\sum_{n=1}^{\infty} U_n^*(\zeta') U_n(\zeta) = \delta(\zeta' - \zeta). \tag{6.46}$$

Applying this equation to the spherical harmonics the completeness relation becomes

$$\sum_{n=0}^{\infty} \sum_{m=-n}^{n} Y_n^m(\theta, \phi) Y_n^m(\theta', \phi')^* = \delta(\phi - \phi')\delta(\cos\theta - \cos\theta'). \tag{6.47}$$

The importance of the spherical harmonics rests in the fact that *any arbitrary function on a sphere* $g(\theta,\phi)$ can be expanded in terms of them,

$$g(\theta,\phi)=\sum_{n=0}^{\infty}\sum_{m=-n}^{n}A_{nm}Y_n^m(\theta,\phi), \tag{6.48}$$

where $A_{nm}$ are complex constants. Because of the orthonormality of these functions the arbitrary constants can be found from

$$A_{nm}=\int d\Omega\, Y_n^m(\theta,\phi)^* g(\theta,\phi), \tag{6.49}$$

where $\Omega$ is the solid angle defined by

$$\int d\Omega \equiv \int_0^{2\pi} d\phi \int_0^{\pi} \sin\theta d\theta.$$

The delta function in spherical coordinates is given by

$$\delta(\vec{r}-\vec{r}')=\frac{1}{r^2}\delta(r-r')\delta(\phi-\phi')\delta(\cos\theta-\cos\theta'), \tag{6.50}$$

where $\vec{r}=(r,\theta,\phi)$ and $\vec{r}'=(r',\theta',\phi')$. It is easily verified that this delta function satisfies the relation

$$\int_0^{2\pi} d\phi \int_0^{\pi} \sin\theta d\theta \int_0^{\infty} r^2\delta(\vec{r}-\vec{r}')\,dr = 1.$$

The two-dimensional delta function on a sphere is simply

$$\delta(\phi-\phi')\delta(\cos\theta-\cos\theta')$$

which integrates to unity over the solid angle.

The following is a table of some of the spherical harmonics.

| $n=0$ & $1$ | $n=2$ |
|---|---|
| $Y_0^0(\theta,\phi)=\frac{1}{\sqrt{4\pi}}$ | $Y_2^{-2}(\theta,\phi)=3e^{-2i\phi}\sqrt{\frac{5}{96\pi}}\sin^2\theta$ |
| $Y_1^{-1}(\theta,\phi)=e^{-i\phi}\sqrt{\frac{3}{8\pi}}\sin\theta$ | $Y_2^{-1}(\theta,\phi)=\frac{3}{2}e^{-i\phi}\sqrt{\frac{5}{24\pi}}\sin 2\theta$ |
| $Y_1^0(\theta,\phi)=\sqrt{\frac{3}{4\pi}}\cos\theta$ | $Y_2^0(\theta,\phi)=\sqrt{\frac{5}{16\pi}}\left(-1+3\cos^2\theta\right)$ |
| $Y_1^1(\theta,\phi)=-e^{i\phi}\sqrt{\frac{3}{8\pi}}\sin\theta$ | $Y_2^1(\theta,\phi)=-\frac{3}{2}e^{i\phi}\sqrt{\frac{5}{24\pi}}\sin 2\theta$ |
| | $Y_2^2(\theta,\phi)=3e^{2i\phi}\sqrt{\frac{5}{96\pi}}\sin^2\theta$ |

(6.51)

| $n=3$ | |
|---|---|
| $Y_3^{-3}(\theta,\phi) = e^{-3i\phi}\sqrt{\frac{35}{64\pi}}\sin^3\theta$ | $Y_3^{1}(\theta,\phi) = e^{i\phi}\sqrt{\frac{21}{64\pi}}\left(1-5\cos^2\theta\right)\sin\theta$ |
| $Y_3^{-2}(\theta,\phi) = 15e^{-2i\phi}\sqrt{\frac{7}{480\pi}}\cos\theta\sin^2\theta$ | $Y_3^{2}(\theta,\phi) = 15e^{2i\phi}\sqrt{\frac{7}{480\pi}}\cos\theta\sin^2\theta$ |
| $Y_3^{-1}(\theta,\phi) = e^{-i\phi}\sqrt{\frac{21}{256\pi}}\left(3+5\cos 2\theta\right)\sin\theta$ | $Y_3^{3}(\theta,\phi) = -\frac{5}{8}e^{3i\phi}\sqrt{\frac{7}{5\pi}}\sin^3\theta$ |
| $Y_3^{0}(\theta,\phi) = \sqrt{\frac{7}{16\pi}}\left(-3\cos\theta+5\cos^3\theta\right)$ | |

(6.52)

Note that for $m = 0$,

$$Y_n^0(\theta,\phi) = \sqrt{\frac{2n+1}{4\pi}}P_n(\cos\theta). \tag{6.53}$$

The simplicity of the spherical harmonics is borne out in the gray-scale plot of the $n = 8$ terms, shown in Fig. 6.5. In this plot the values of $\mathrm{Re}[Y_n^m(\theta,\phi)]$ $(m = 0, 1, \cdots, 8)$ on a unit sphere are projected onto the $(y, z)$ plane, looking down the positive $x$ axis, using a gray scale with white the most positive and black the most negative in the mapping of the value of the function. The nodal lines are drawn in along with the outline of the sphere. The gray background outside the sphere is the color mapped to zero. The beauty and simplicity of the spherical harmonics is illustrated very well in this kind of plot. Note that $Y_8^0$ has no longitudinal nodal lines, whereas $Y_8^1$ has its longitudinal nodal lines on the great circle corresponding with the circle outline.

## 6.4 Radial Functions

### 6.4.1 Spherical Bessel Functions

We can rewrite Eq. (6.10) as

$$[\frac{d^2}{dr^2} + \frac{2}{r}\frac{d}{dr} + k^2 - \frac{n(n+1)}{r^2}]R_n(r) = 0. \tag{6.54}$$

This would be Bessel's equation, Eq. (4.32), except for the coefficient of $2/r$ instead of $1/r$. However, we transform Eq. (6.54) to Bessel's equation with the substitution,

$$R_n(r) = \frac{1}{r^{1/2}}u_n(r) \tag{6.55}$$

yielding

$$[\frac{d^2}{dr^2} + \frac{1}{r}\frac{d}{dr} + k^2 - \frac{(n+1/2)^2}{r^2}]u_n(r) = 0. \tag{6.56}$$

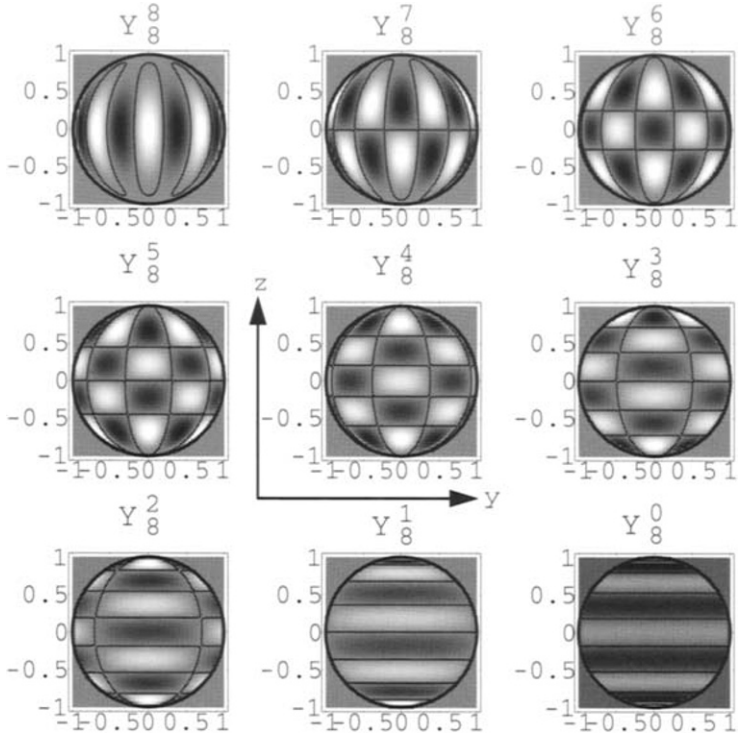


**Figure 6.5:** $n$=8 spherical harmonics viewed looking down the $x$-axis. The real part is plotted in gray scale and the nodal lines are indicated by the thin solid lines.

The solutions of Eq. (6.56) are Bessel functions $J_{n+1/2}(kr)$ and $Y_{n+1/2}(kr)$ or the corresponding Hankel functions. Note that the wavenumber $k$ appears alone in the argument now (whereas in cylindrical coordinates we had $\sqrt{k^2 - k_z^2}$). Thus Eq. (6.55) leads us to the following solution of Eq. (6.54).

$$R_n(r) = \frac{A_n}{r^{1/2}} J_{n+1/2}(kr) + \frac{B_n}{r^{1/2}} Y_{n+1/2}(kr).$$

The spherical Bessel and Hankel functions are defined in terms of these solutions:

$$\begin{aligned}
j_n(x) &\equiv (\frac{\pi}{2x})^{1/2} J_{n+1/2}(x) \\
y_n(x) &\equiv (\frac{\pi}{2x})^{1/2} Y_{n+1/2}(x) \\
h_n^{(1)}(x) &\equiv j_n(x) + iy_n(x) = (\frac{\pi}{2x})^{1/2} [J_{n+1/2}(x) + iY_{n+1/2}(x)] \\
h_n^{(2)}(x) &\equiv j_n(x) - iy_n(x) = (\frac{\pi}{2x})^{1/2} [J_{n+1/2}(x) - iY_{n+1/2}(x)].
\end{aligned} \tag{6.57}$$

Note that when $x$ is real

$$h_n^{(2)}(x) = (h_n^{(1)}(x))^*. \tag{6.58}$$

Figures 6.6 and 6.7 show plots of $j_n(x)$ and $y_n(x)$. respectively, for $n = 0, 2, 4, 6$.

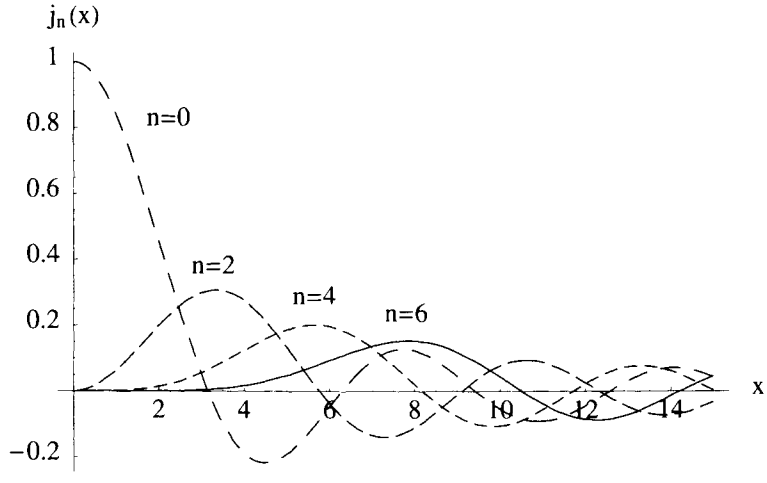


**Figure 6.6:** Spherical Bessel functions, $j_n(x)$ for $n = 0, 2, 4, 6$.

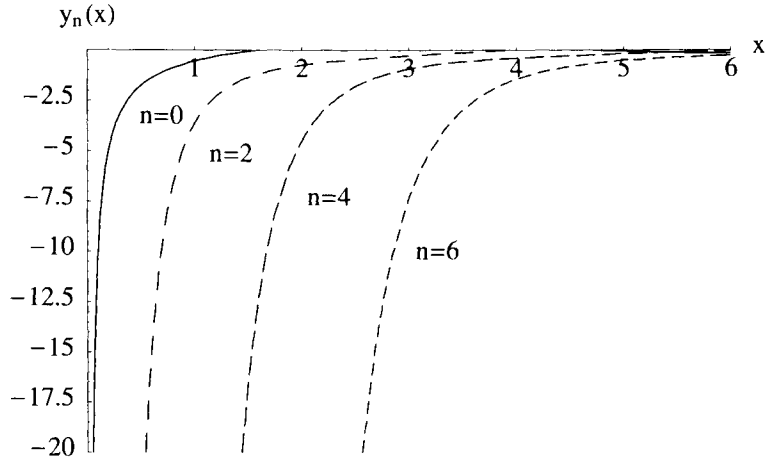


**Figure 6.7:** Spherical Bessel functions $y_n(x)$ for $n = 0, 2, 4, 6$.

It is important to realize that, unlike the Bessel functions of integer argument, simple expressions exist for the spherical Bessel functions in terms of trigonometric functions.

These are written concisely as

$$\begin{aligned} j_n(x) &= (-x)^n(\frac{1}{x}\frac{d}{dx})^n(\frac{\sin x}{x}) \\ y_n(x) &= -(-x)^n(\frac{1}{x}\frac{d}{dx})^n(\frac{\cos x}{x}) \\ h_n^{(1)}(x) &= (-x)^n(\frac{1}{x}\frac{d}{dx})^n(\frac{e^{ix}}{ix}) \\ &= (-x)^n(\frac{1}{x}\frac{d}{dx})^n[h_0^{(1)}(x)]. \end{aligned} \tag{6.59}$$

The first few relationships are

$$\begin{aligned} j_0(x) &= \frac{\sin x}{x} \\ j_1(x) &= -\frac{\cos x}{x} + \frac{\sin x}{x^2} \\ j_2(x) &= \frac{-\sin x}{x} - \frac{3\cos x}{x^2} + \frac{3\sin x}{x^3} \\ j_3(x) &= \frac{\cos x}{x} - \frac{6\sin x}{x^2} - \frac{15\cos x}{x^3} + \frac{15\sin x}{x^4}, \end{aligned} \tag{6.60}$$

$$\begin{aligned} y_0(x) &= -\frac{\cos x}{x} \\ y_1(x) &= -\frac{\sin x}{x} - \frac{\cos x}{x^2} \\ y_2(x) &= +\frac{\cos x}{x} - \frac{3\sin x}{x^2} - \frac{3\cos x}{x^3} \\ y_3(x) &= \frac{\sin x}{x} + \frac{6\cos x}{x^2} - \frac{15\sin x}{x^3} - \frac{15\cos x}{x^4}, \end{aligned} \tag{6.61}$$

and

$$\begin{aligned} h_0^{(1)}(x) &= \frac{e^{ix}}{ix} \\ h_1^{(1)}(x) &= -\frac{e^{ix}\,(i+x)}{x^2} \\ h_2^{(1)}(x) &= \frac{i\,e^{ix}\left(-3+3\,i\,x+x^2\right)}{x^3} \\ h_3^{(1)}(x) &= \frac{e^{ix}\left(-15\,i-15\,x+6\,i\,x^2+x^3\right)}{x^4}. \end{aligned} \tag{6.62}$$

The behavior near the origin of the coordinate system is given by the small argument expressions for the spherical Bessel functions ($x << n$):

$$j_n(x) \approx \frac{x^n}{(2n+1)!!}(1 - \frac{x^2}{2(2n+3)} + \cdots), \tag{6.63}$$

$$\begin{aligned} y_n(x) &\approx -\frac{(2n-1)!!}{x^{n+1}}(1 - \frac{x^2}{2(1-2n)} + \cdots), \\ h_n(x) &\approx -i\frac{(2n-1)!!}{x^{n+1}} \\ h_n'(x) &\approx i\frac{(n+1)(2n-1)!!}{x^{n+2}} \end{aligned} \tag{6.64}$$

where $(2n+1)!! = (2n+1)(2n-1)(2n-3)\cdots 3 \cdot 1$. A useful relation is

$$(2n+1)!! = \frac{(2n+1)!}{2^n n!}. \tag{6.65}$$

It is clear from these expansions that, as with the cylindrical Bessel functions, only the $j_n$ functions are finite at the origin, and only $j_0$ is non-zero there.

Two useful Wronskian relations are

$$j_n(x)y_n'(x) - j_n'(x)y_n(x) = \frac{1}{x^2}, \tag{6.66}$$

and

$$j_n(x)h_n^{'(1)}(x) - j_n'(x)h_n^{(1)}(x) = \frac{i}{x^2}. \tag{6.67}$$

The large argument limits of the spherical Hankel functions are given by the first term (the $1/x$ term) in Eqs (6.60–6.62). In particular,

$$\begin{aligned} h_n^{(1)}(x) &\approx (-i)^{n+1}\frac{e^{ix}}{x}, \\ h_n'(x) &\approx (-i)^n\frac{e^{ix}}{x}. \end{aligned} \tag{6.68}$$

A set of recurrence relations exist for the spherical Bessel and Hankel functions. In particular,

$$\begin{aligned} \frac{2n+1}{x}h_n(x) &= h_{n-1}(x) + h_{n+1}(x) \\ h_n'(x) &= h_{n-1}(x) - \frac{n+1}{x}h_n(x). \end{aligned} \tag{6.69}$$

In Eq. (6.69) one can replace $h_n$ with either $j_n$, $y_n$ or $h_n^{(2)}$ due to the fact that $h_n^{(1)} = j_n + iy_n$ and equating real and imaginary parts.

## 6.5 Multipoles

Radiation from bodies which are located at the origin and which are of finite extent can be characterized by sums of multipoles. Multipole expansions are similar to (but not identical to) the spherical harmonic expansions with the corresponding outgoing radial functions:

$$p(r,\theta,\phi,\omega) = \sum_{n=0}^{\infty}\sum_{m=-n}^{n} C_{mn}h_n^{(1)}(kr)Y_n^m(\theta,\phi), \tag{6.70}$$

where $r$ is greater than or equal to the largest radial extent of the body. There is not, however, a one-to-one correspondence between the multipoles and the terms in the series in Eq. (6.70). Multipoles are constructed from distributions of point sources, infinitesimally close to the origin, of equal amplitudes but opposite phases. Whereas the spherical harmonics are orthogonal to one another, the multipoles are not. In any case, we will show that the $n = m = 0$ term in Eq. (6.70) does correspond to the simplest multipole, the monopole, and the $n = 1$ terms to the dipoles.

### 6.5.1 Monopoles

Consider first the simplest multipole, a point source located at the origin called a monopole. The radiated pressure associated with it is omnidirectional (independent of angle) and, if $Q_s$ is its source strength (volume flow), then its pressure is given by

$$p = \frac{-i\rho_0 ck}{4\pi} Q_s \frac{e^{ikr}}{r}. \tag{6.71}$$

Note that due to Eq. (6.62)

$$\frac{e^{ikr}}{r} = ikh_0(kr)$$

so that the monopole is the $n = 0$, $m = 0$ term of Eq. (6.70):

$$p(r, \theta, \phi) = C_{00} \frac{1}{\sqrt{4\pi}} h_0(kr).$$

Comparing this to Eq. (6.71) reveals that

$$C_{00} = \frac{\rho_0 ck^2}{\sqrt{4\pi}} Q_s.$$

To develop expressions for the dipoles and quadrupoles we need to represent combinations of point sources located near the origin. To this end consider a point source located at $r = r'$.[5] The Helmholtz equation is

$$\nabla^2 G(\mathbf{r}|\mathbf{r}') + k^2 G(\mathbf{r}|\mathbf{r}') = -\delta(\mathbf{r} - \mathbf{r}'), \tag{6.72}$$

where both $\mathbf{r}$ and $\mathbf{r}'$ are measured from the origin and

$$G(\mathbf{r}|\mathbf{r}') = \frac{e^{ikR}}{4\pi R} = \frac{ik}{4\pi} h_0(kR). \tag{6.73}$$

The bold face quantities represent vector quantities (so that $\vec{r} \equiv \mathbf{r}$, $\vec{r}' \equiv \mathbf{r}'$) and

$$R^2 \equiv |\mathbf{r} - \mathbf{r}'|^2 = (x - x')^2 + (y - y')^2 + (z - z')^2. \tag{6.74}$$

Thus the radiated pressure at the field point $\mathbf{r}$, in view of Eq. (6.71), is

$$p(\mathbf{r}|\mathbf{r}') = -i\rho_0 ckQ_s G(\mathbf{r}|\mathbf{r}'). \tag{6.75}$$

[5] P. M. Morse and K. U. Ingard (1968). *Theoretical Acoustics*. McGraw-Hill, New York, pp. 310–314.

This is a monopole located at $\mathbf{r}'$.

We can compute the average energy density ($\mathbf{v}$ is a velocity vector) at a field point $\mathbf{r}$ for any of the multipoles using the general relation[6]

$$e_{av} = \frac{1}{4}\rho_0 \mathbf{v}\cdot\mathbf{v}^* + \frac{1}{4}\frac{|p|^2}{\rho_0 c^2}. \tag{6.76}$$

It is instructive to write the expressions for the radial velocity, average energy density, intensity, and power radiated by a monopole source from the pressure field given by Eq. (6.71).[7] The radial velocity from Euler's equation is

$$\begin{aligned} \dot{w} &= \frac{1}{i\rho_0 ck}\frac{\partial p}{\partial r} = -\frac{ikQ_s}{4\pi}\frac{e^{ikr}}{r}\left(1-\frac{1}{ikr}\right) \\ &= \frac{p}{\rho_0 c}\left(1+\frac{i\lambda}{2\pi r}\right). \end{aligned} \tag{6.77}$$

Unlike the pressure the radial velocity has a nearfield associated with it, defined by the additional $1/ikr$ term. As $kr$ increases this nearfield becomes negligible. From Eq. (6.76) the average energy density is

$$e_{av} = \frac{\rho_0 k^2 |Q_s|^2}{(4\pi r)^2}\left(\frac{1}{2}+\frac{1}{4(kr)^2}\right). \tag{6.78}$$

The three components of the average acoustic intensity are provided by Eq. (2.16), page 19:

$$\begin{aligned} I_r &= \frac{|Q_s|^2}{2}\frac{\rho_0 ck^2}{(4\pi r)^2} = \frac{|p|^2}{2\rho_0 c}, \\ I_\phi &= 0 \\ I_\theta &= 0. \end{aligned} \tag{6.79}$$

Finally, the total power defined by $\Pi = \int I_r r^2 d\Omega$ is

$$\Pi = (4\pi r^2) I_r = \frac{\rho_0 ck^2}{8\pi}|Q_s|^2. \tag{6.80}$$

These relations contrast the nearfield and farfield regions of the monopole.

### 6.5.2 Dipoles

Next we consider the representation of a dipole. A dipole consists of two point sources opposite in phase and separated by an infinitesimal distance $d$ oriented along one of the rectangular coordinate axes. Consider the axial dipole as shown in Fig. 6.8. We define

[6] A. Pierce (1981). *Acoustics: An Introduction to Its Physical Principles and Applications.* McGraw-Hill, New York, p. 40 Eq. (1-11.11a).

[7] P. M. Morse and K. U. Ingard (1968). *Theoretical Acoustics.* McGraw-Hill, New York, p. 311.

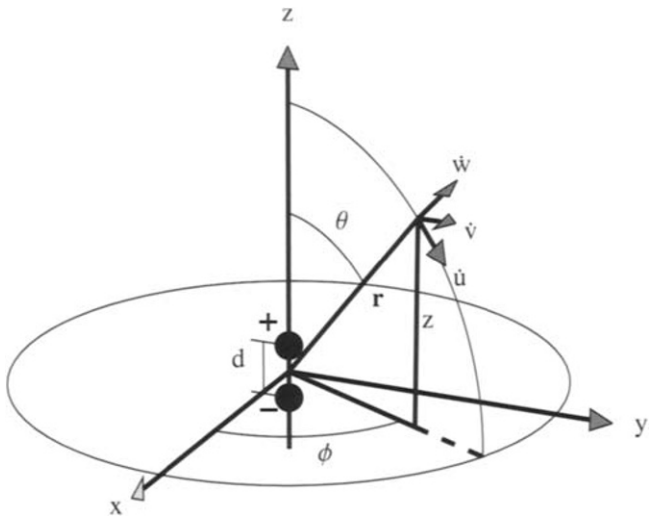


**Figure 6.8:** Dipole along the $z$ axis. The positive source is at $\mathbf{r}' = \mathbf{d}/2$ and the negative point source is at $\mathbf{r}' = -\mathbf{d}/2$. The field point, $\mathbf{r}$, shows the orientations of the three components of the velocity vector.

the dipole strength, $D_s = Q_s d$, and assume that $d$ is vanishingly small. Two point sources of opposite phase, as shown in Fig. 6.8, create a pressure

$$\begin{aligned} p(r,\theta,\phi) &= -i\rho_0 ckQ_s[G(\mathbf{r}|\frac{1}{2}\mathbf{d}) - G(\mathbf{r}|-\frac{1}{2}\mathbf{d})] \\ &= -i\rho_0 ckQ_s d\frac{\partial G}{\partial z'}\Big|_{\mathbf{r}'=0} \\ &= -\rho ck^2 D_s \cos\theta(1+\frac{i}{kr})\frac{e^{ikr}}{4\pi r}. \end{aligned} \tag{6.81}$$

Because the dipole was oriented along the $z$ axis the pressure field is independent of $\phi$. Unlike the monopole there is a nearfield pressure associated with the dipole. Also the pressure field depends on $\cos\theta$. The two non-zero components of velocity are

$$\begin{aligned} \dot{w} &= -k^2 D_s \cos\theta\left(1+\frac{2i}{kr}-\frac{2}{(kr)^2}\right)\frac{e^{ikr}}{4\pi r}, \\ \dot{u} &= -ikD_s \sin\theta\left(1+\frac{i}{kr}\right)\frac{e^{ikr}}{4\pi r^2}. \end{aligned} \tag{6.82}$$

The average energy density is

$$e_{av} = \frac{\rho_0}{2}\left(\frac{k^2 D_s}{4\pi r}\right)^2\left[\frac{1}{2}\left(\frac{1}{(kr)^2}+\frac{1}{(kr)^4}\right)+\left(1+\frac{3}{2(kr)^4}\right)\cos^2\theta\right]. \tag{6.83}$$

The only non-zero active intensity component is the radial intensity given by

$$I_r = \frac{\rho_0 c k^4 |D_s|^2 \cos^2\theta}{2(4\pi r)^2}. \tag{6.84}$$

Whereas the monopole power is proportional to the square of the frequency, the total power for the dipole is proportional to the fourth power:

$$\Pi = \frac{\rho_0 c k^4 |D_s|^2}{24\pi}. \tag{6.85}$$

If the dipole is along the $x$ axis then the positive and negative sources create a pressure field given by

$$p = -i\rho_0 c k Q_s d \frac{\partial G}{\partial x'}\Big|_{\mathbf{r}'=0}. \tag{6.86}$$

Evaluating the partial derivative and using Eq. (6.1) leads to the angle factor $\sin\theta\cos\phi$ which is proportional to $\mathrm{Re}[Y_1^1]$. The dipole oriented along the $y$ axis turns out to have an angle factor of $\sin\theta\sin\phi$ which is proportional to $\mathrm{Im}[Y_1^1]$. The directivity patterns of the three dipoles are shown in Fig. 6.9.

To relate the dipole pressure field to the spherical harmonic expansion, Eq. (6.70), we need to recast Eq. (6.81) in terms of Hankel functions. From Eq. (6.59)

$$h_n(kR) = -(\frac{R}{k})^n (\frac{1}{R}\frac{d}{dR})^n [h_0(kR)]. \tag{6.87}$$

We can see that a dipole is generated if $n = 1$ in Eq. (6.87) since this leads to the first derivative of $h_0(kR)$, the latter being a monopole source. That is, since

$$G = \frac{ik}{4\pi} h_0(kR)$$

and $R = |\mathbf{r} - \mathbf{r}'|$, then $\frac{\partial G}{\partial z'}$ in Eq. (6.81) is

$$\frac{\partial G}{\partial z'}\Big|_{\mathbf{r}'=0} = \frac{\partial h_0(kR)}{\partial z'}\Big|_{\mathbf{r}'=0} = \frac{d}{dR} h_0(kR) \frac{\partial R}{\partial z'}\Big|_{\mathbf{r}'=0} = -k h_1(kr)\cos\theta.$$

Note that $\cos\theta = \sqrt{4\pi/3} Y_1^0$ (see Eq. (6.52)) so that, returning to Eq. (6.70), we see that the axial dipole corresponds to the $m = 0$, $n = 1$ term of the general spherical harmonic expansion and thus can be represented by a single spherical harmonic. Note that the $x$ and $y$ oriented dipoles are both constructed from the $m = 1$, $n = 1$ term using the real and imaginary parts of $Y_1^1$, respectively.

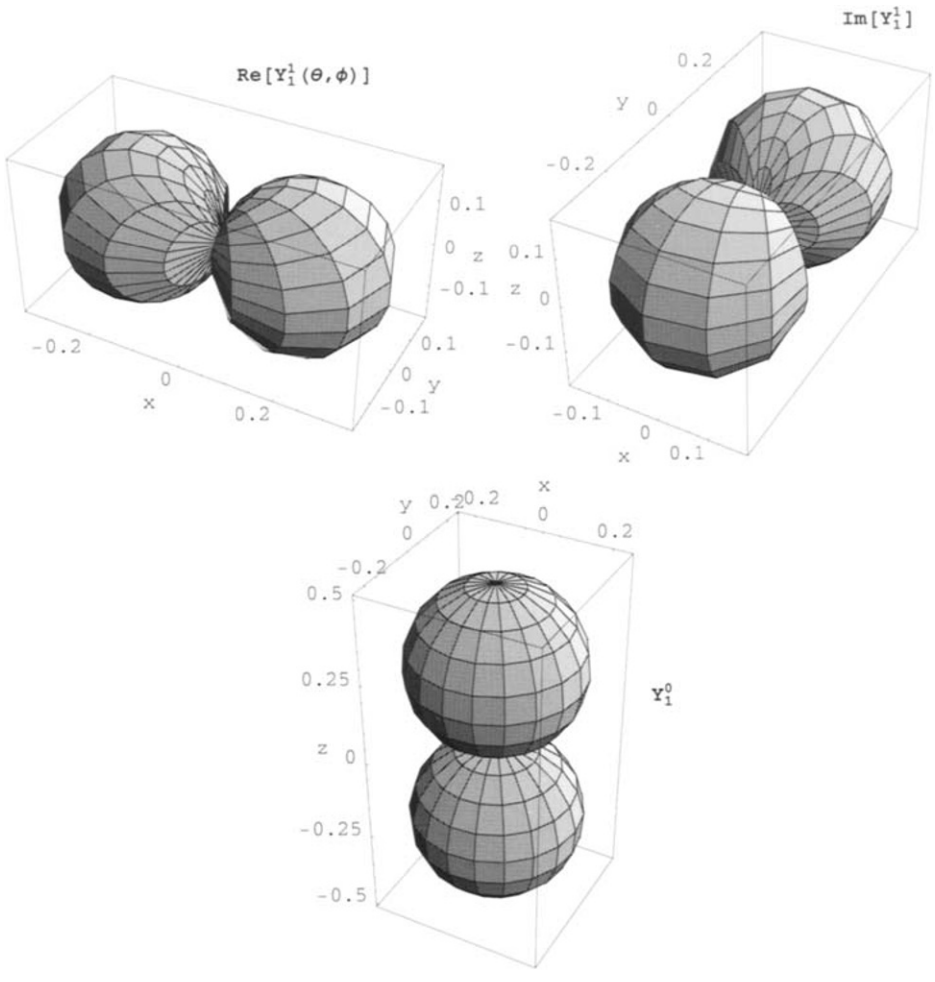


**Figure 6.9:** Angular dependence of the pressure field generated by the three dipoles.

### 6.5.3 Quadrupoles

Opposing orientations of dipoles lead to quadrupoles with strengths $Q_s d^2$. The pressure due to the configuration shown in Fig. 6.10 is

$$p = -i\rho_0 ckQ_{xy}[\frac{\partial^2}{\partial x' \partial y'} G(\mathbf{r}|\mathbf{r}')]\Big|_{r'=0}, \tag{6.88}$$

with the two opposing dipoles placed in the $(x, y)$ plane. Using analysis similar to the dipole case it turns out that this pressure is proportional to $h_2(kr)$ and the imaginary part of $Y_2^2(\theta, \phi)$. The angular dependence of this quadrupole is shown in the left-top plot of Fig. 6.11, labeled $\mathrm{Im}[Y_2^2]$. Note the pressure field vanishes on the coordinate

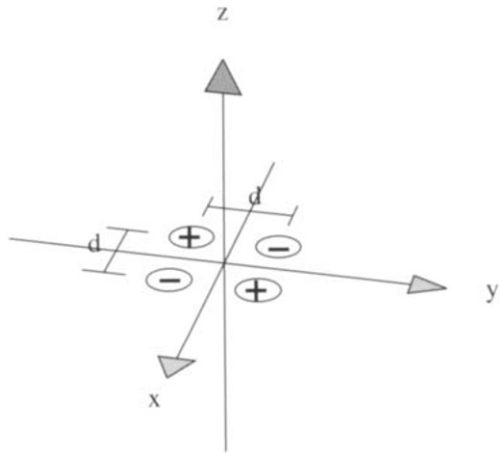


**Figure 6.10:** Two opposing dipoles in the $(x, y)$ plane which form a quadrupole.

axes. Similarly, two opposing dipoles in the $(x, z)$ plane lead to the real part of $Y_2^1$, and in the $(y, z)$ plane to the imaginary part of $Y_2^1$ as shown in the right plot in the figure.

It is interesting to compute the so called longitudinal quadrupole, given by

$$[\frac{\partial^2}{\partial z'^2} G(\mathbf{r}|\mathbf{r}')]\Big|_{r'=0}.$$

We find that this is nearly equal to $Y_2^0(\theta)$ (see Fig. 6.11 for $Y_2^0$) except that we need to subtract a monopole term from it in order to arrive at the correct pressure field of a longitudinal quadrupole. This points out the important fact that the terms of Eq. (6.70) do not have a one-to-one correspondence with multipoles. In fact, multipoles are not even orthogonal, but are built out of terms in the spherical harmonic series of Eq. (6.70).

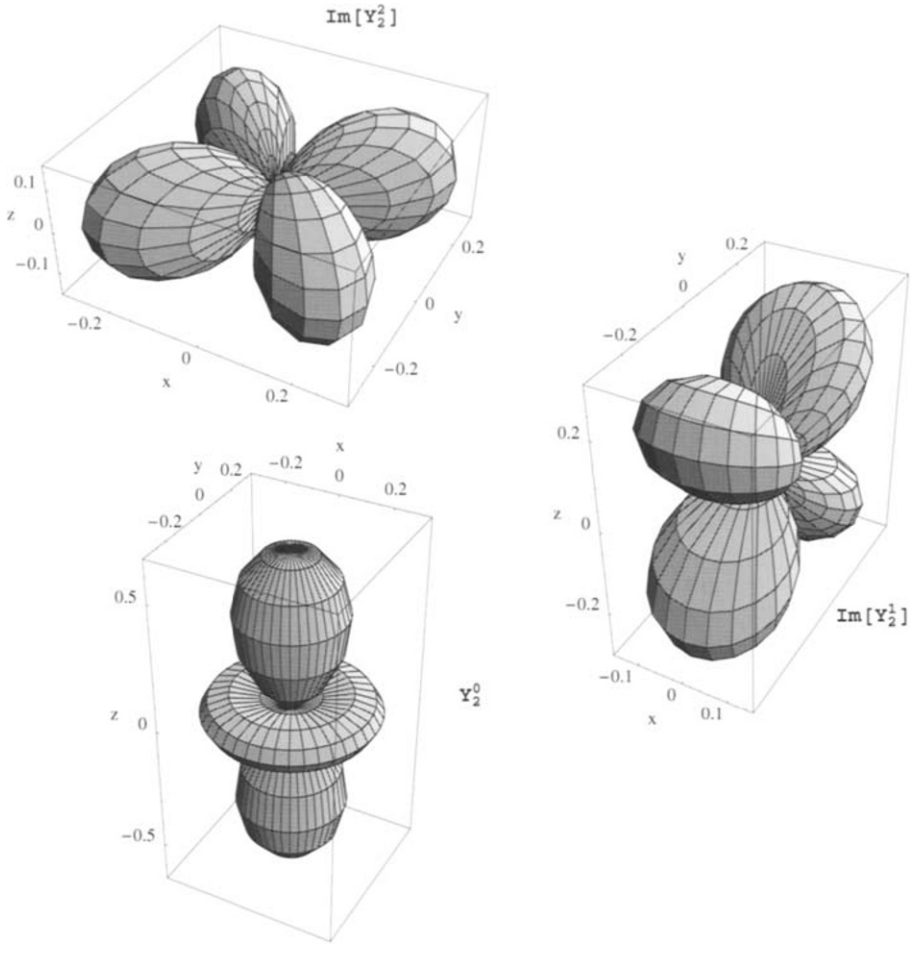


**Figure 6.11:** Farfield directivity patterns for the $n = 2$ spherical harmonics.

## 6.6 Spherical Harmonic Directivity Patterns

As we have seen with plates and cylinders the farfield directivity pattern is defined by removing the $e^{ikr}/r$ factor so that the directivity pattern $D(\theta, \phi)$ is defined by

$$\lim_{r\to\infty}[p(r,\theta,\phi)] = \frac{e^{ikr}}{r}D(\theta,\phi). \tag{6.89}$$

Note that the expansion in Eq. (6.70) differs from the functions in cylindrical and planar coordinates in that the directivity pattern is explicitly part of the wave functions. That is, from Eq. (6.70)

$$D(\theta,\phi) = \lim_{r\to\infty}[re^{-ikr}h_n(kr)]\Upsilon_n^m(\theta,\phi). \tag{6.90}$$

Using Eq. (6.68) the directivity pattern of the $(n, m)$th spherical harmonic is

$$D(\theta, \phi) = \frac{(-i)^{n+1}}{k} Y_n^m(\theta, \phi). \tag{6.91}$$

The spherical harmonics provide the farfield directivity pattern of each term in the series, Eq. (6.70). This exposes the remarkable fact that for each spherical harmonic the nodes of pressure which arise from $P_n^m(\cos\theta)$ extend uninterrupted from the origin to the farfield.

The directivity patterns for some of the higher order spherical harmonics are shown in Figs 6.12 and 6.13. The first of these figures represents the patterns for the $Y_3^m$ harmonics, and the second figure the $Y_4^m$ harmonics. We have plotted the absolute value of the imaginary parts ($\phi$ dependence is $\sin(m\phi)$). The vertical axis is the $z$ axis. Note that Fig. 6.11 provided, in similar fashion, the $Y_2^m$ directivity patterns.

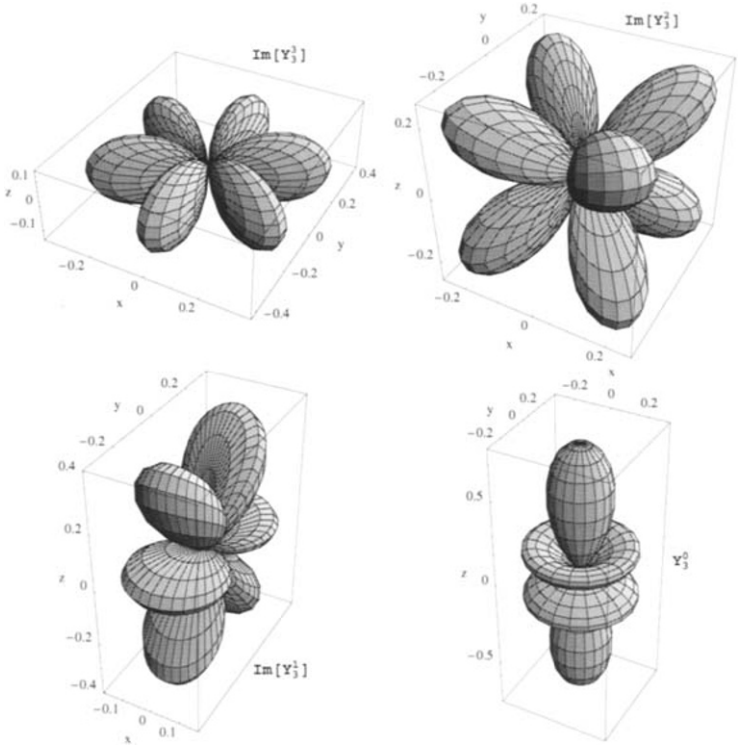


**Figure 6.12:** Farfield directivity patterns for the $n = 3$ spherical harmonics. The absolute value of the imaginary part of $Y_n^m$ is plotted which leads to a $\sin(m\phi)$ dependence in $\phi$.

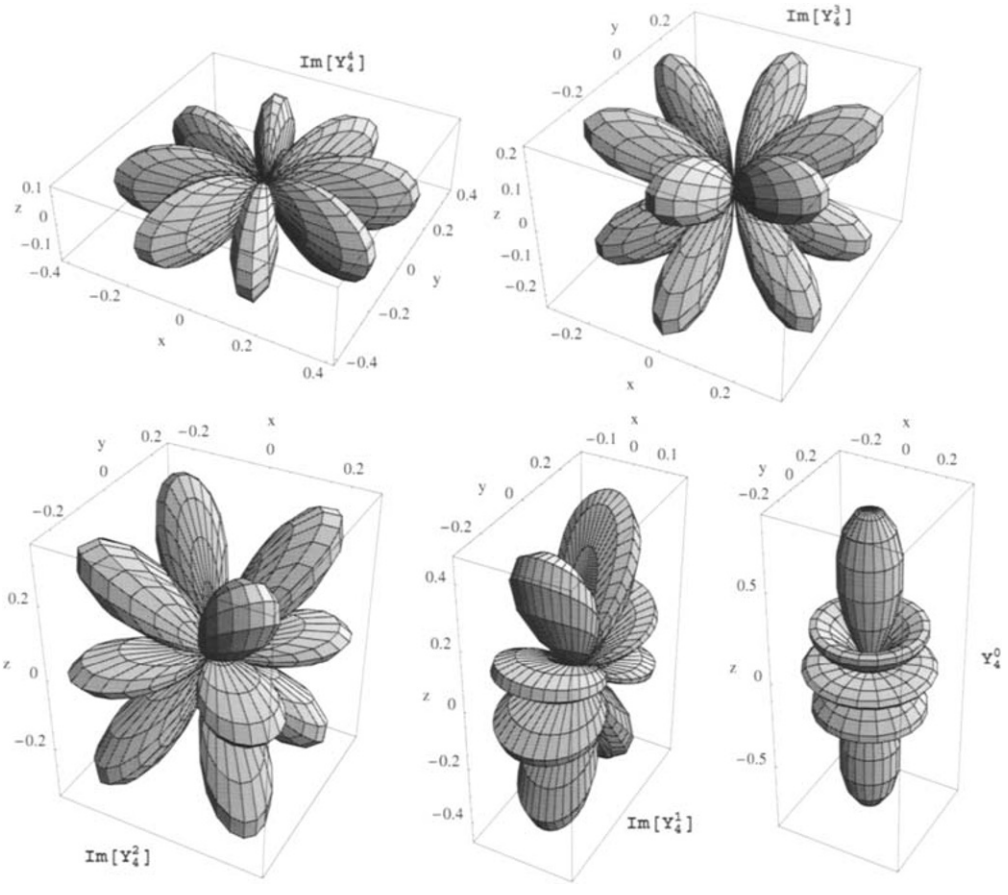


**Figure 6.13:** Farfield directivity patterns for the $n = 4$ spherical harmonics. The absolute value of the imaginary part of $Y_n^m$ is plotted which leads to a $\sin(m\phi)$ dependence in $\phi$.

## 6.7 General Solution for Exterior Problems

The exterior domain is defined as shown in Fig. 6.14. The sphere of radius $a$ is the smallest sphere tangent to the outermost extremity of the source and does not cut through the source at any point.

Equation (6.70) applies to this problem and the radiated pressure field is given by

$$p(r,\theta,\phi,\omega) = \sum_{n=0}^{\infty} \sum_{m=-n}^{n} C_{mn}(\omega) h_n(kr) Y_n^m(\theta,\phi). \tag{6.92}$$

The radiated pressure field is completely defined when the coefficients $C_{mn}$ are determined. The $C_{mn}$ are generally functions of frequency. The spherical Hankel function

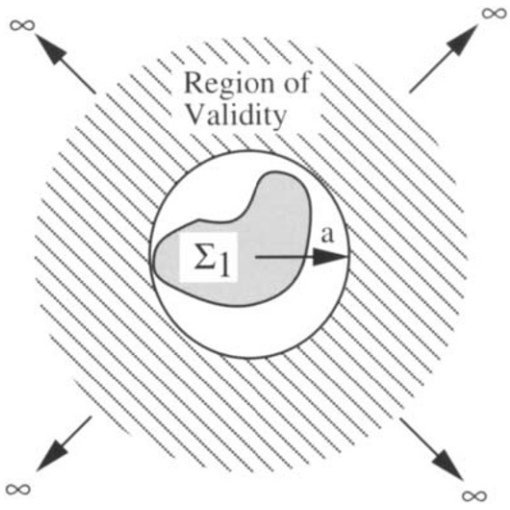


**Figure 6.14:** Exterior domain problem with all sources inside the spherical surface at $r = a$.

$h_n(kr)$ stands for the outgoing definition, $h_n^{(1)}(kr)$. As was the case with the plate and the cylinder, if the pressure field is known on a separable surface (a sphere) of the coordinate system then the three-dimensional field outside the source can be easily determined, as we will now show.

Assume that the pressure $p(r, \theta, \phi)$ is known on a sphere of radius $r = a$. The complete three-dimensional field is uniquely defined if the coefficients $C_{mn}$ can be determined. We determine the coefficients by using the orthonormal property of the spherical harmonics. To this end multiply each side of Eq. (6.92) (evaluated at $r = a$) by $Y_q^p(\theta, \phi)^*$ and integrate over the surface of a unit sphere. The result is

$$C_{mn} = \frac{1}{h_n(ka)} \iint p(a, \theta, \phi) \Upsilon_n^m(\theta, \phi)^* \sin\theta \, d\theta \, d\phi. \tag{6.93}$$

Inserting this result into Eq. (6.92) yields the complete solution,

$$p(r, \theta, \phi) = \sum_{n=0}^{\infty} \frac{h_n(kr)}{h_n(ka)} \sum_{m=-n}^{n} \Upsilon_n^m(\theta, \phi) \int p(a, \theta', \phi') \Upsilon_n^m(\theta', \phi')^* d\Omega', \tag{6.94}$$

where $d\Omega' = \sin\theta' d\theta' d\phi'$. This important equation relates the pressure on a sphere of radius $a$ to the radiated pressure on a sphere of radius $r$.

### 6.7.1 Spherical Wave Spectrum

Just as we define the plane wave spectrum for plane waves and the helical wave spectrum for cylindrical waves, we define the spherical wave spectrum $P_{mn}(r)$ at $r = r_0$ as

$$P_{mn}(r_0) \equiv \int p(r_0, \theta, \phi) \Upsilon_n^m(\theta, \phi)^* d\Omega. \tag{6.95}$$

which decomposes the pressure on the sphere of radius $r_0$ into its spherical wave components. For comparison the helical and plane wave spectra were given in Eq. (4.52) on page 125 and Eq. (2.52) on page 32, respectively. For the sphere the wave is defined by Eq. (6.20) and thus is composed of a traveling wave component in $\phi$ using $e^{im\phi}$ and a standing wave component in $\theta$ given by $P_n^m(\cos\theta)$. Because of the standing wave component we can not define wave fronts, as we did with the plane and cylindrical spectra. One could expand the Legendre functions into traveling wave components using $\cos\theta = (e^{i\theta} + e^{-i\theta})/2$ to develop expressions purely in terms of traveling waves $(e^{im\phi+in\theta})$. This may be useful in some problems but it is rarely done in the literature, and we will not pursue it any further here.

One can make an analogy to "$k$-space" where the wavenumbers $k_x$ and $k_y$ are imitated by $m/r_0$ and $n/r_0$. At times we will refer to the spherical wave spectrum as a $k$-space spectrum because of this analogy.

As was done for planar and cylindrical systems we can view Eq. (6.95) as a forward Fourier transform using $Y_n^m(\theta,\phi)$ as the basis function. The corresponding inverse Fourier transform (a double Fourier series) is just

$$p(r,\theta,\phi) = \sum_{n=0}^{\infty} \sum_{m=-n}^{n} P_{mn}(r) Y_n^m(\theta,\phi), \tag{6.96}$$

due to the orthonormality of the basis functions. Comparison with Eq. (6.94) reveals that

$$P_{mn}(r) = \frac{h_n(kr)}{h_n(kr_0)} P_{mn}(r_0), \tag{6.97}$$

which provides wavefield extrapolation very similar to the cylindrical wave case given in Eq. (4.58) on page 126. When $r \geq r_0$ the extrapolation is a forward one, and when $r < r_0$ it is an inverse one, equivalent in the time domain to going back in time. The latter is the realm of spherical NAH which will be discussed in the next chapter.

### 6.7.2 The Relationship Between Velocity and Pressure Spectra

First we define the spherical wave spectrum for the radial velocity $\dot{W}_{mn}$:

$$\dot{W}_{mn}(r) \equiv \int \dot{w}(r,\theta,\phi) Y_n^m(\theta,\phi)^* d\Omega, \tag{6.98}$$

associated with the inverse relationship,

$$\dot{w}(r,\theta,\phi) = \sum_{n=0}^{\infty} \sum_{m=-n}^{n} \dot{W}_{mn}(r) Y_n^m(\theta,\phi). \tag{6.99}$$

Euler's equation, Eq. (6.5), applied to Eq. (6.96) with $\frac{dP_{mn}(r)}{dr}$ derived from Eq. (6.97) yields

$$\dot{w}(r,\theta,\phi) = \frac{1}{i\rho_0 c} \sum_{n=0}^{\infty} \sum_{m=-n}^{n} \frac{h_n'(kr)}{h_n(kr_0)} P_{mn}(r_0) Y_n^m(\theta,\phi). \tag{6.100}$$

Comparison with Eq. (6.99) shows that the relationship between the velocity and pressure spectra is

$$\dot{W}_{mn}(r) = \frac{1}{i\rho_0 c}\frac{h_n'(kr)}{h_n(kr_0)}P_{mn}(r_0), \tag{6.101}$$

or equivalently

$$P_{mn}(r_0) = i\rho_0 c\frac{h_n(kr_0)}{h_n'(kr)}\dot{W}_{mn}(r). \tag{6.102}$$

Similar to the cylinder (Eq. (4.71), page 133), the definition of the specific acoustic impedance $Z_{mn}$ is

$$Z_{mn} \equiv \frac{P_{mn}(r_0)}{\dot{W}_{mn}(r_0)} = i\rho_0 c\frac{h_n(kr_0)}{h_n'(kr_0)}. \tag{6.103}$$

### 6.7.3 Evanescent Waves

The wavelength in the $\phi$ direction is dictated by $m$ since $Y_n^m \propto e^{im\phi}$. Thus $m$ counts the number of full wavelengths in the circumferential direction around the sphere. Of course the actual wavelength is largest around the equator, and diminishes as we move towards the poles. This would seem to imply that the acoustic short circuit is greater at the poles producing stronger evanescence. On the contrary, however, the radial decay, given by the ratio of Hankel functions in Eq. (6.97), is independent of latitude. Thus the wavefunction in the polar angle must somehow compensate for this increased acoustic short circuit near the poles. That is, the wavelength in the $\theta$ direction depends on $m$, in such a way that the spherical harmonic $Y_n^m$ possesses the same radial decay for all permissible values of $m$, and the acoustic short circuit is equalized so that it is independent of latitude.

Study of Figs 6.3 and 6.4 reveals the dependency with respect to the polar angle $\theta$. In this case, as the figures indicate, the number of "half-wavelengths" from $\theta = 0$ to $\theta = \pi$ is given by $n - m + 1$. (Note that the leading term of the series expansion for $P_n^m$ given in Eq. (6.30) is $\cos^{n-m}\theta$.) These "half-wavelengths" are a bit peculiar since they are not strictly sinusoidal, as the figures show. At the poles the standing waves taper smoothly to zero. The half-wavelength near the poles is greater than the half-wavelength at the equator. These two effects, or peculiarities, would appear to compensate to some degree for the increased acoustic short circuit due to the vanishing circumferential wavelength near the poles. Also note that for fixed $n$ the number of these "half-wavelengths" increases when $m$ decreases and vice versa. This is reminiscent of the behavior of plane and helical waves. That is, in $k$-space we learned that a circle defined a set of waves which have the same attenuation (if subsonic) or phase relation (if supersonic) in the normal direction to the surface. As we move around the $k$-space circle the wavelength in one direction diminishes while the wavelength in the perpendicular direction increases. Reference back to Fig. 6.5 should clarify these statements. In this case $n = 8$ and all the "modes" shown undergo the same radial decay when evanescent.

Returning to Eq. (6.97) we see that the ratio of Hankel functions dictates how the spherical wave spectrum components change phase and amplitude from one sphere to another. We can understand the asymptotic behavior of evanescent waves by studying

the behavior when $kr_0 << n$ and $kr << n$. Using Eq. (6.64) we have

$$\frac{h_n(kr)}{h_n(kr_0)} \approx (r_0/r)^{n+1}, \tag{6.104}$$

a power law decay similar to the cylindrical evanescent wave case. This evanescent behavior is greatest when $r - r_0$ is small, since as $r$ increases the condition $kr << n$ breaks down and we must take more terms in the small argument expansion for the Hankel function.

### 6.7.4 Boundary Value Problem with Specified Radial Velocity

As we have done with the plate and the cylinder, we want to find a relationship between the radial velocity on the inner sphere at $r = a$ and the pressure on any spherical surface $r > a$. We have derived the relationship in $k$-space between pressure and normal velocity, given in Eq. (6.102). If we insert this equation into Eq. (6.96) we obtain

$$p(r,\theta,\phi) = i\rho_0 c \sum_{n=0}^{\infty} \frac{h_n(kr)}{h_n'(ka)} \sum_{m=-n}^{n} \dot{W}_{mn}(a) Y_n^m(\theta,\phi). \tag{6.105}$$

Finally we use Eq. (6.98) for $\dot{W}_{mn}(a)$:

$$p(r,\theta,\phi) = i\rho_0 c \sum_{n=0}^{\infty} \frac{h_n(kr)}{h_n'(ka)} \sum_{m=-n}^{n} Y_n^m(\theta,\phi) \int \dot{w}(a,\theta',\phi') Y_n^m(\theta',\phi')^* d\Omega', \tag{6.106}$$

where $d\Omega' = \sin\theta' d\theta' d\phi'$.

Solving boundary value problems is a simple two-step process. With the normal surface velocity prescribed over the whole boundary, Eq. (6.98) is used to compute the velocity spectrum, $\dot{W}_{mn}(a)$. This spectrum is inserted into Eq. (6.105) to solve for the pressure on any sphere of radius $r \geq a$.

### 6.7.5 The Rayleigh-like Integrals

Rayleigh's first integral formula, Eq. (2.75) on page 36, relates the radiated pressure to surface velocity for plates. The expression for cylinders was given by Eq. (4.77) on page 134. For spheres we can express the Rayleigh-like integral as[8]

$$p(r,\theta,\phi) = i\rho_0 ck a^2 \int G_N(r,\theta,\phi|a,\theta',\phi') \dot{w}(a,\theta',\phi') d\Omega'. \tag{6.107}$$

where $G_N$ is called a Neumann Green function which will be discussed in more detail in a later chapter. Comparison of this equation with Eq. (6.106) reveals the expression for $G_N$:

$$G_N(r,\theta,\phi|a,\theta',\phi') = \frac{1}{ka^2} \sum_{n=0}^{\infty} \frac{h_n(kr)}{h_n'(ka)} \sum_{m=-n}^{n} Y_n^m(\theta,\phi) Y_n^m(\theta',\phi')^*. \tag{6.108}$$

[8] M. C. Junger and D. Feit (1986). *Sound, Structures, and Their Interaction*. 2nd ed. MIT Press, Cambridge, MA. p. 157.

Note that Eq. (6.107) is no longer a convolution, as it was for plates.

The 2nd Rayleigh-like integral, which relates pressures on two boundaries, is

$$p(r,\theta,\phi) = -a^2 \int G_D(r,\theta,\phi|a,\theta',\phi')p(a,\theta',\phi')\,d\Omega', \tag{6.109}$$

where $G_D$ is the Dirichlet Green function, derived from Eq. (6.94). That is,

$$G_D(r,\theta,\phi|a,\theta',\phi') = \frac{-1}{a^2}\sum_{n=0}^{\infty}\frac{h_n(kr)}{h_n(ka)}\sum_{m=-n}^{n} Y_n^m(\theta,\phi)Y_n^m(\theta',\phi')^*. \tag{6.110}$$

When $r = a$, the ratio of spherical Hankel functions is unity and the double sum is a delta function, Eq. (6.47), and the integral reduces to an identity.

### 6.7.6 Radiated Power

The radiated power is computed from the integral of the radial acoustic intensity (time averaged) over any sphere outside the source regions:

$$\Pi(\omega) = \frac{1}{2}\iint \mathrm{Re}[p(r_0,\theta,\phi)\dot{w}^*(r_0,\theta,\phi)]r_0^2\sin\theta\,d\theta\,d\phi, \tag{6.111}$$

where $r_0$ is the radius of the sphere. From Eq. (6.92) and Euler's equation, Eq. (6.5), we have

$$\dot{w}(r_0,\theta,\phi) = \frac{1}{i\rho_0 ck}\frac{\partial p}{\partial r} = \frac{1}{i\rho_0 c}\sum_{n=0}^{\infty}\sum_{m=-n}^{n} C_{mn}(\omega)h_n'(kr_0)Y_n^m(\theta,\phi). \tag{6.112}$$

Inserting this result into Eq. (6.111), using Eq. (6.45) yields

$$\Pi = \frac{r_0^2}{2}\sum_{m.n}|C_{mn}|^2 Re[\frac{h_n(kr_0)h_n'(kr_0)^*}{i\rho_0 c}].$$

This expression is simplified by writing $h_n = j_n + iy_n$ and using the Wronskian relationship given in Eq. (6.66). It reduces to

$$\Pi = \frac{1}{2\rho_0 ck^2}\sum_{n=0}^{n}\sum_{m=-n}^{n}|C_{mn}|^2. \tag{6.113}$$

Thus the sum over the squared magnitude weights of each of the spherical harmonics provides the power radiated to the farfield. There is no power coupling between spherical harmonics of different orders. On the other hand, the active intensity in the nearfield is composed of coupled spherical harmonics.

### 6.7.7 Farfield Pressure

The farfield for Eq. (6.106) or Eq. (6.105) is easily obtained from the farfield expression for the spherical Hankel function, Eq. (6.68):

$$p(r,\theta,\phi) \approx \rho_0 c\frac{e^{ikr}}{kr}\sum_{n=0}^{\infty}\frac{(-i)^n}{h_n'(ka)}\sum_{m=-n}^{n}\dot{W}_{mn}Y_n^m(\theta,\phi). \tag{6.114}$$

### Farfield Low Frequency Result

We use the fact that (see Eq. (6.64))

$$\lim_{x\to 0} h_n(x) = -i\frac{(2n-1)!!}{x^{n+1}},$$

and

$$\lim_{x\to 0} h_0'(x) = \frac{i}{x^2}$$

in Eq. (6.114) to obtain to leading order (the $n = 0$ term dominates):

$$p(r,\theta,\phi) \approx -i\rho_0 ckA^2\frac{e^{ikr}}{r}\dot{W}_{00}Y_0^0(\theta,\phi)$$

so that

$$\lim_{k\to 0} p(r,\theta,\phi,\omega) = -i\rho_0 ckA^2\frac{e^{ikr}}{4\pi r}\int_0^{2\pi} d\phi' \int_0^{\pi} \dot{w}(a,\theta',\phi')\sin\theta' d\theta'. \tag{6.115}$$

Note that the double integral is proportional to the total volume flow ($m^3/s$) $Q_s$:

$$Q_s \equiv a^2\int_0^{2\pi} d\phi' \int_0^{\pi} \dot{w}(a,\theta',\phi')\sin\theta' d\theta', \tag{6.116}$$

so that the radiated pressure at low frequencies is

$$\lim_{k\to 0} p(r,\theta,\phi,\omega) = -i\rho_0 ckQ_s\frac{e^{ikr}}{4\pi r}. \tag{6.117}$$

Comparison to Eq. (6.71) reveals that at low frequencies the leading term in the farfield pressure is a monopole, with source strength $Q_s$.

### High Frequency Result

An interesting result is obtained in the high frequency limit, in which case both the spherical Hankel functions in the numerator and denominator of Eq. (6.106) can be approximated by their asymptotic expressions. Using Eq. (6.68) we find that

$$\lim_{k\to\infty} p(r,\theta,\phi) = \rho_0 ca\frac{e^{ik(r-a)}}{r}\int \dot{w}(a,\theta',\phi')\sum_{n=-\infty}^{\infty}\sum_{m=-n}^{n} Y_n^m(\theta,\phi)Y_n^m(\theta',\phi')^* d\Omega'.$$

The double sum can be simplified by use of Eq. (6.47), replacing them with delta functions. The integration of solid angle is then trivial yielding $\dot{w}(a,\theta,\phi)$. The final result is

$$\lim_{k\to\infty} p(r,\theta.\phi) = \rho_0 ca\frac{e^{ik(r-a)}}{r}\dot{w}(a,\theta,\phi). \tag{6.118}$$

This equation makes the significant statement that in the short wavelength limit the given velocity at any point on the sphere at $r = a$ maps to the farfield following the ray projecting radially outward at the same spherical angle.

### 6.7.8 Radiation from a Pulsating Sphere

As an example of the application of Eq. (6.106), we consider a pulsating sphere (constant radial velocity). The sphere has a radius $a$ and is vibrating uniformly radially at a frequency $\omega$ such that

$$\dot{w}(a,\theta,\phi) = \dot{W}.$$

Recognizing the fact that $\dot{W} = \sqrt{4\pi}Y_0^0\dot{W}$ then

$$\int \dot{w}(a,\theta',\phi')Y_n^m(\theta',\phi')^* d\Omega' = \dot{W}\int \sqrt{4\pi}Y_0^0 Y_n^m(\theta',\phi')^* d\Omega' = \sqrt{4\pi}\dot{W}\delta_{m0}\delta_{n0}.$$

Then Eq. (6.106) becomes, using Eq. (6.62).

$$p(r,\theta,\phi) = i\rho_0 c\frac{h_0(kr)}{h_0'(ka)}Y_0^0\sqrt{4\pi}\dot{W} = \rho_0 c\dot{W}ka^2\frac{ka-i}{((ka)^2+1)r}e^{ik(r-a)}. \tag{6.119}$$

When the pulsating sphere is very small compared to a wavelength, $ka << 1$, then the surface pressure is almost 90 degrees out of phase with the surface velocity,

$$p(r) \approx -i\rho_0 cka^2\dot{W}\frac{e^{ikr}}{r}. \tag{6.120}$$

Clearly the pulsating sphere becomes a point source in this limit with source strength $Q_s = 4\pi a^2\dot{W}$.

At very high frequencies, $ka >> 1$, the pressure and velocity are in phase and we have

$$p(r) \approx \rho_0 ca\dot{W}\frac{e^{ik(r-a)}}{r}. \tag{6.121}$$

Note there is no restriction on $r$ in these relations, except that $r \geq a$, thus they are valid in the near and farfield.

### 6.7.9 General Axisymmetric Source

We can use Eq. (6.106) to derive the general formula relating surface velocity to exterior pressure for an axisymmetric source which is defined through

$$\dot{w}(a,\theta,\phi) = \dot{w}(a,\theta) \tag{6.122}$$

(is independent of $\phi$). This is equivalent to specifying $m = 0$ for the azimuthal functions $e^{im\phi}$. Using Eq. (6.53)

$$p(r,\theta) = i\rho_o c\sum_{n=0}^{\infty}\frac{(2n+1)}{2}\frac{h_n(kr)}{h_n'(ka)}P_n(\cos\theta)\int_0^{\pi}\dot{w}(a,\theta')P_n(\cos\theta')\sin\theta' d\theta'. \tag{6.123}$$

For a given surface velocity we solve for the radiated pressure by first expanding the surface velocity in Legendre polynomials. Since the $m = 0$ polynomials form a complete set, the expansion is

$$\dot{w}(a,\theta') = \sum_{p=0}^{\infty}\dot{W}_p P_p(\cos\theta'), \tag{6.124}$$

so that Eq. (6.123) becomes (using the orthogonality relations, Eq. (6.28))

$$p(r,\theta) = i\rho_o c \sum_{n=0}^{\infty} \dot{W}_n \frac{h_n(kr)}{h_n'(ka)} P_n(\cos\theta). \tag{6.125}$$

We determine the coefficients $\dot{W}_n$ by multiplying Eq. (6.124) by $P_p(\cos\theta)$ and integrating over $\theta$:

$$\dot{W}_n = \frac{2n+1}{2} \int_0^{\pi} \dot{w}(a,\theta') P_n(\cos\theta') \sin\theta' \, d\theta'. \tag{6.126}$$

**Farfield Pressure**

The farfield is obtained as for the nonaxisymmetric case, using Eq. (6.68), so that Eq. (6.125) becomes

$$\lim_{r\to\infty} p(r,\theta) = \rho_o c \frac{e^{ikr}}{kr} \sum_{n=0}^{\infty} \dot{W}_n \frac{(-i)^n}{h_n'(ka)} P_n(\cos\theta). \tag{6.127}$$

**High Frequency Case**

As we did for the general case resulting in Eq. (6.118), we can use the asymptotic expansions for the Hankel functions in Eq. (6.127) so that

$$\lim_{k\to\infty} p(r,\theta) = \rho_0 c \frac{a}{r} e^{ik(r-a)} \int_0^{\pi} \dot{w}(a,\theta') \sum_{n=0}^{\infty} \frac{2n+1}{2} P_n(\cos\theta) P_n(\cos\theta') \sin\theta' d\theta'.$$

We need the completeness relation, Eq. (6.46), for Legendre polynomials. In this case

$$U_n(x) = \sqrt{\frac{2n+1}{2}} P_n(x), \tag{6.128}$$

so that

$$\sum_{n=0}^{\infty} \frac{2n+1}{2} P_n(x') P_n(x) = \delta(x'-x). \tag{6.129}$$

Finally,

$$\lim_{k\to\infty} p(r,\theta) = \rho_0 c \frac{a}{r} e^{ik(r-a)} \dot{w}(a,\theta), \tag{6.130}$$

which, of course, agrees with Eq. (6.118) for the general case. Again the velocity beams radially outward in the high frequency limit.

## 6.7.10 Circular Piston in a Spherical Baffle

As an example of an axisymmetric source we compute the radiation from a circular (spherical cap) piston on an otherwise rigid sphere. The piston is placed at the pole so that we can make the problem axisymmetric and use the axisymmetric formulation presented above. Figure 6.15 shows the geometry.

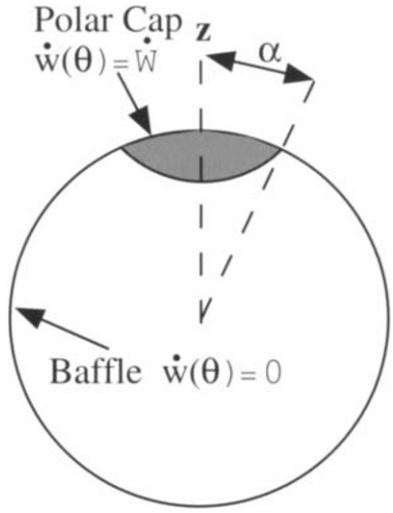


**Figure 6.15:** Circular piston of radius $\alpha$ set in a rigid sphere. The piston vibrates with a velocity $\dot{W}$. The $z$ axis passes through the center of the piston.

The velocity on the sphere (independent of $\phi$) is

$$\begin{aligned} \dot{w}(a,\theta) &= \dot{W}, \qquad 0 \le \theta \le \alpha \\ &= 0, \qquad \alpha < \theta \le \pi. \end{aligned}$$

Equation (6.125) provides the radiated pressure. We compute the coefficients $\dot{W}_n$ from Eq. (6.126):

$$\dot{W}_n = \frac{(2n+1)}{2}\dot{W}\int_0^\alpha P_n(\cos\theta)\sin\theta\, d\theta = \frac{(2n+1)}{2}\dot{W}\int_{\cos\alpha}^1 P_n(\eta)d\eta. \tag{6.131}$$

To evaluate this integral we need one of the recurrence formulas for the Legendre polynomials,[9]

$$(2n+1)P_n(\eta) = \frac{dP_{n+1}}{d\eta} - \frac{dP_{n-1}}{d\eta}, \tag{6.132}$$

where, when $n = 0$, only the first term on the right is used. Thus

$$\dot{W}_n = \frac{\dot{W}}{2}[P_{n-1}(\cos\alpha) - P_{n+1}(\cos\alpha)], \tag{6.133}$$

since $P_{n-1}(1) = P_{n+1}(1) = 1$. For $n = 0$ we have $\dot{W}_0 = (1 - \cos\alpha)/2$. Finally using Eq. (6.125):

$$p(r,\theta) = \frac{i\rho_o c\dot{W}}{2}\sum_{n=0}^{\infty}[P_{n-1}(\cos\alpha) - P_{n+1}(\cos\alpha)]\frac{h_n(kr)}{h_n'(ka)}P_n(\cos\theta), \tag{6.134}$$

[9] J. D. Jackson (1975). *Classical Electrodynamics*, 2nd ed. Wiley & Sons, p. 89.

where it is understood that for $n = 0$ the difference of Legendre polynomials is just $1 - \cos\alpha$.

### 6.7.11 Point Source on a Baffle

We let $\alpha$ become infinitesimally small so that Eq. (6.131) can be written ($P_n \approx 1$)

$$\dot{W}_n = \frac{2n+1}{2}\dot{W}\int_0^\alpha \theta\, d\theta = \frac{2n+1}{4}\alpha^2\dot{W}.$$

Given that the area of the point source is $\pi a^2\alpha^2$, the source produces a volume flow of

$$Q_s = \pi a^2\alpha^2\dot{W},$$

and we can write

$$\dot{W}_n = \frac{2n+1}{4\pi a^2}Q_s.$$

The pressure field at any range is given by Eq. (6.125):

$$p(r,\theta) = \frac{i\rho_0 cQ_s}{4\pi a^2}\sum_{n=0}^{\infty}(2n+1)\frac{h_n(kr)}{h_n'(ka)}P_n(\cos\theta). \tag{6.135}$$

In the farfield we use Eq. (6.127) to obtain,

$$\lim_{r\to\infty} p(r,\theta) = -\frac{i\rho_o ckQ_s}{4\pi}\frac{e^{ikr}}{r}\sum_{n=0}^{\infty}\frac{(-i)^{n-1}(2n+1)}{(ka)^2h_n'(ka)}P_n(\cos\theta). \tag{6.136}$$

We recognize the coefficient multiplying the sum as the pressure radiated from a point source in free space with no baffle:

$$p_f(r) \equiv -\frac{i\rho_o ckQ_s}{4\pi}\frac{e^{ikr}}{r}, \tag{6.137}$$

and write Eq. (6.136) as

$$\lim_{r\to\infty} p(r,\theta) = p_f(r)\sum_{n=0}^{\infty}\frac{(-i)^{n-1}(2n+1)}{(ka)^2h_n'(ka)}P_n(\cos\theta). \tag{6.138}$$

The low frequency result, keeping the first two terms, is

$$\lim_{r\to\infty} p(r,\theta) \approx p_f(r)(1 - i\frac{3ka}{2}\cos\theta), \tag{6.139}$$

which gives us some clue as to the effect of the circular baffle on the radiation from the point source. Due to the $\cos\theta$ the second term is a dipole. Comparison to Eq. (6.81) reveals that the dipole moment is $D_s = 3aQ_s/2$. At very low frequencies the second term is negligible and $p \to p_f$, that is, the baffle has no effect.

In Fig. 6.16 we plot the farfield pressure as a function of polar angle for four cases, $ka = 1, 5, 10, 20$, using Eq. (6.136).

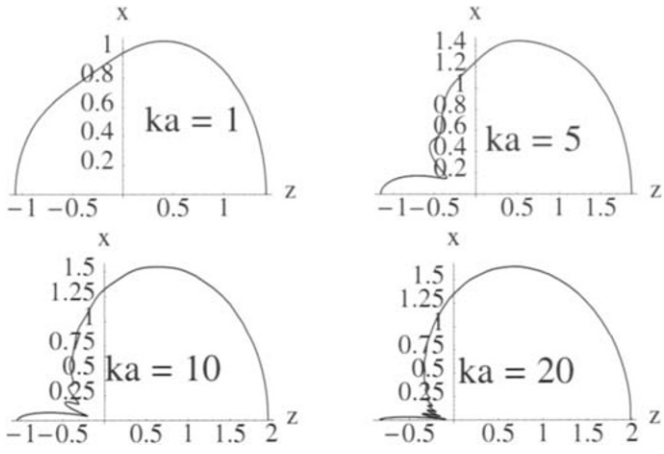


**Figure 6.16:** Farfield for a point source on the north pole of a rigid sphere as a function of polar angle measured from the horizontal ($z$) axis. The sphere shadows the point source as the frequency increases.

## 6.8 General Solution for Interior Problems

For the interior problem the sources are located outside a sphere of radius $r = b$ as shown in Fig. 6.17. The solution consists of radial functions which are finite at the

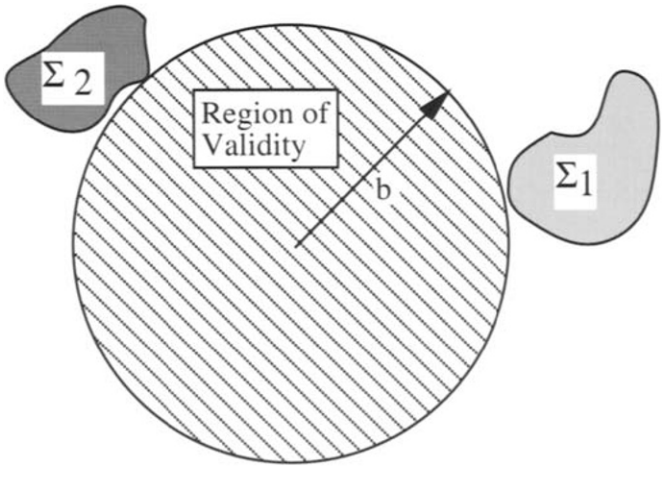


**Figure 6.17:** Region of validity for the interior solution. Sources are located outside the region defined by $r \geq b$.

origin, so that the internal pressure field is, in general,

$$p(r,\theta,\phi,\omega) = \sum_{n=0}^{\infty} \sum_{m=-n}^{n} A_{mn}(\omega) j_n(kr) Y_n^m(\theta,\phi). \tag{6.140}$$

As we had in Eq. (6.93),

$$A_{mn} = \frac{1}{j_n(kb)} \int \int p(b,\theta,\phi) Y_n^m(\theta,\phi)^* \sin\theta \, d\theta \, d\phi. \tag{6.141}$$

Inserting this result into Eq. (6.140) yields the complete solution,

$$p(r,\theta,\phi) = \sum_{n=0}^{\infty} \frac{j_n(kr)}{j_n(kb)} \sum_{m=-n}^{n} Y_n^m(\theta,\phi) \int p(b,\theta',\phi') Y_n^m(\theta',\phi')^* d\Omega', \tag{6.142}$$

where $d\Omega' = \sin\theta' d\theta' d\phi'$. This important equation relates the pressure on a sphere of radius $b$ to the pressure inside.

In "$k$-space" the spectral components, instead of Eq. (6.97), become

$$P_{mn}(r) = \frac{j_n(kr)}{j_n(kr_0)} P_{mn}(r_0), \tag{6.143}$$

where $P_{mn}$ is defined in Eq. (6.95). In this case, when $r \leq r_0 \leq b$ the problem is a forward one, and when $b \geq r > r_0$ an inverse one. We will study the latter case in detail in Chapter 7.

### 6.8.1 Radial Surface Velocity Specified

If the radial velocity is specified on the surface at $r = b$ then Eq. (6.5) and Eq. (6.140) lead to

$$\dot{w}(a,\theta,\phi) = \frac{1}{i\rho_0 c} \sum_{n=0}^{\infty} \sum_{m=-n}^{n} A_{mn}(\omega) j_n'(kb) Y_n^m(\theta,\phi). \tag{6.144}$$

As we did with Eq. (6.92) we invert this equation to solve for the unknown coefficients $A_{mn}$ to obtain,

$$A_{mn} = \frac{i\rho_0 c}{j_n'(kb)} \int \dot{w}(b,\theta',\phi') Y_n^m(\theta',\phi')^* d\Omega'. \tag{6.145}$$

Finally inserting Eq. (6.145) into Eq. (6.140) yields,

$$p(r,\theta,\phi) = i\rho_0 c \sum_{n=0}^{\infty} \frac{j_n(kr)}{j_n'(kb)} \sum_{m=-n}^{n} Y_n^m(\theta,\phi) \int \dot{w}(b,\theta',\phi') Y_n^m(\theta',\phi')^* d\Omega'. \tag{6.146}$$

We can also write this in the two-step form,

$$\dot{W}_{mn}(b) \equiv \int \dot{w}(b,\theta',\phi') Y_n^m(\theta',\phi')^* d\Omega'. \tag{6.147}$$

and

$$p(r,\theta,\phi) = i\rho_0 c \sum_{n=0}^{\infty} \frac{j_n(kr)}{j_n'(kb)} \sum_{m=-n}^{n} \dot{W}_{mn}(b) Y_n^m(\theta,\phi). \tag{6.148}$$

These results are very similar to the results Eq. (6.106), Eq. (6.98), and Eq. (6.105), for the exterior problem.

The spherical wave spectrum ("$k$-space") for the exterior problem was given in Eq. (6.102). For the interior case we have

$$P_{mn}(r) = i\rho_0 c \frac{j_n(kr)}{j_n'(kr_0)} \dot{W}_{mn}(r_0), \tag{6.149}$$

where $r_0 \leq b$ and $r \leq b$.

Using the definition for $\dot{W}_{mn}(b)$ (Eq. (6.147)) in Eq. (6.148) leads to the Rayleigh-like integral

$$p(r,\theta,\phi) = i\rho_0 ckb^2 \int G_N(r,\theta,\phi|b,\theta',\phi') \dot{w}(b,\theta',\phi') d\Omega', \tag{6.150}$$

where the Neumann Green function is defined similar to Eq. (6.107) as

$$G_N(r,\theta,\phi|b,\theta',\phi') \equiv \frac{1}{kb^2} \sum_{n=0}^{\infty} \frac{j_n(kr)}{j_n'(kb)} \sum_{m=-n}^{n} Y_n^m(\theta,\phi) Y_n^m(\theta',\phi')^*, \tag{6.151}$$

and $r \leq b$.

Although these results are very similar in form to the ones for the exterior problem, there are some fundamental differences which arise. We are now dealing with a finite domain instead of an infinite one so we expect resonances to occur in the interior space. These resonances or interior eigenfrequencies occur when the denominator of Eq. (6.151) or Eq. (6.142) is zero. To illuminate the issue we will solve the pulsating sphere problem (Section 6.7.8) again, this time for the interior field.

### 6.8.2 Pulsating Sphere

Consider a pulsating sphere with the boundary condition ($e^{-i\omega t}$ time dependence) on its surface,

$$\dot{w}(b,\theta,\phi) = \dot{W}.$$

Using Eq. (6.147)

$$\dot{W}_{mn}(b) = \sqrt{4\pi}\dot{W}\delta_{m0}\delta_{n0}.$$

Thus Eq. (6.148) yields, using Eq. (6.59),

$$p(r) = i\rho_0 c \frac{j_0(kr)}{j_0'(kb)} \dot{W} = -i\rho_0 c \frac{j_0(kr)}{j_1(kb)} \dot{W}. \tag{6.152}$$

The denominator of Eq. (6.152) is plotted in Fig. 6.18 below, Every zero crossing corresponds to an infinite pressure in Eq. (6.152) for all $r \leq b$, that is, an antiresonance of the interior space. In terms of the acoustic impedance, with $p(r)$ evaluated at $r = b$,

$$Z_{ac} \equiv p(b)/\dot{W}; \tag{6.153}$$

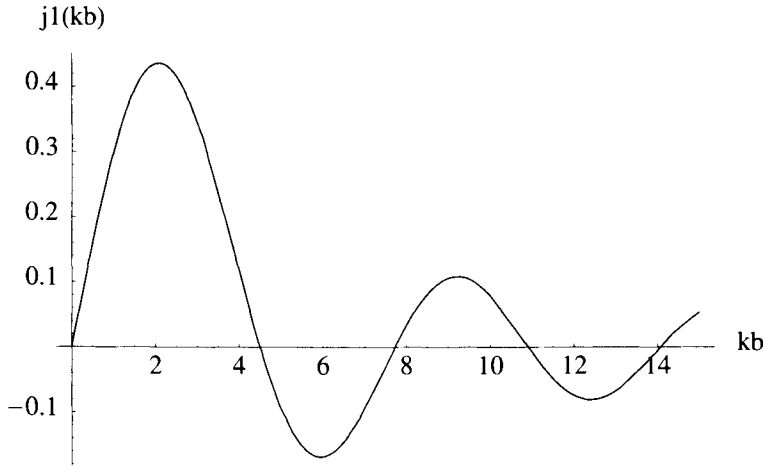


**Figure 6.18:** Plot of $j_1(kb)$.

the impedance becomes infinite at these zero crossings, and thus the motion of the sphere encounters an infinite force opposing its attempt to oscillate. Since the motion is blocked by the infinite force we call it an antiresonance, not a resonance. We can see from Eq. (6.60), as $kb$ becomes large that the zeros of $j_1$ are solutions of $\cos(kb) = 0$ or

$$kb = \frac{\pi}{2}(2n+1), \quad n = 1, 2, 3 \cdots.$$

This translates to antiresonance frequencies

$$\omega_n = \frac{\pi c}{2b}(2n+1). \tag{6.154}$$

On the other hand the numerator of Eq. (6.152) has an infinite number of zeros given by the zeros of $j_0(kb)$, when $r = b$. These occur exactly when $\sin(kb) = 0$ or

$$\omega_n = \frac{\pi c n}{b}, \quad n = 1, 2, 3 \cdots,$$

and since $p = 0$ on the surface we call these frequencies resonances. That is, the surface has no force opposing its motion. The resonance and antiresonance frequencies alternate. This definition of resonance is consistent with that for a spring-mass system, if we view the fluid inside the sphere as the mass and spring, and the spherical boundary as the other end of the spring. When this end is vibrated (with velocity $\dot{w}$), the reaction force goes to zero at resonance (the mass and spring are in violent motion at the other end). Conversely, at antiresonance the force is infinite and the mass is motionless, corresponding to zero internal pressure.

### Low Frequency Result

As $k \to 0$ then from Eq. (6.63)

$$\frac{j_0(kb)}{j_1(kb)} \to 3/kb,$$

and Eq. (6.152) yields

$$p(b) = -i\rho_0 c\frac{3}{kb}\dot{W} = -i\rho_0 c^2\frac{3}{\omega b}\dot{W} = \frac{3B}{i\omega b}\dot{W}, \tag{6.155}$$

where $B$ is the bulk modulus (stiffness of the fluid) defined by

$$c = \sqrt{B/\rho_0}. \tag{6.156}$$

Define a spring constant $K$ through

$$F = \frac{K}{-i\omega}\dot{W}.$$

where $F$ is the outward force (in Newtons) and $\dot{W}$ the velocity, or rate of change of the compression of the spring. Since positive pressure represents compression, and thus an inward force squeezing the fluid, the force $F = -4\pi b^2 p(b)$. Thus the internal fluid represents a spring of stiffness $K$ from Eq. (6.155) given by

$$K = 12\pi bB. \tag{6.157}$$

The "bubble" acts as a spring at low frequencies, and is completely reactive. As the frequency increases we keep the second term in the expansion of $j_0(kb)$ which gives rise to a mass term which resonates with this spring to create the first resonance at $kb = \pi$ or $\omega_1 = \pi c/b$.

## 6.9 Transient Radiation - Exterior Problems

Because of the simplicity of the radial functions, it is possible to solve for the time-dependent pressure radiated from a spherical source with temporal boundary conditions. Assume that the surface velocity in the time domain is given by $\dot{w}_t(a,\theta,\phi,t)$ where we use the subscript $t$ to represent time domain quantities so as to distinguish from the frequency domain. We will assume that $\dot{w}_t(a,\theta,\phi,t) = 0$ for $t < 0$. We solve the transient problem by transforming to the frequency domain so that we can use the expressions relating pressure and velocity, derived in this chapter. Equation (1.7), page 2, defines the temporal inverse Fourier transform:

$$\dot{w}_t(a,\theta,\phi,t) = \frac{1}{2\pi}\int_{-\infty}^{\infty}\dot{w}(a,\theta,\phi,\omega)e^{-i\omega t}d\omega.$$

We can rewrite Eq. (6.105) taking the inverse Fourier transform of both sides as

$$p_t(r,\theta,\phi,t) = i\rho_0 c\sum_{n=0}^{\infty}\sum_{m=-n}^{n}Y_n^m(\theta,\phi)\frac{1}{2\pi}\int_{-\infty}^{\infty}\frac{h_n(\omega r/c)}{h_n'(\omega a/c)}\dot{W}_{mn}(\omega)e^{-i\omega t}d\omega, \tag{6.158}$$

with the "$k$-space" velocity given by

$$\dot{W}_{mn}(\omega) = \int d\Omega' Y_n^{m*}(\theta',\phi')\int\dot{w}_t(a,\theta',\phi',t)e^{i\omega t}dt. \tag{6.159}$$

The frequency integral in Eq. (6.158) is not difficult to evaluate since the Hankel functions are just polynomial-like expressions. We illustrate this by a simple case.

### 6.9.1 Radiation from an Impulsively Moving Sphere

Given $v$ and $\alpha$ constants, let the surface velocity be given by

$$\begin{aligned} \dot{w}_t(a,\theta,t) = ve^{-\alpha t}Y_1^0 &= \sqrt{\frac{3}{4\pi}}ve^{-\alpha t}\cos\theta, \quad t \geq 0, \\ &= 0, \quad t < 0. \end{aligned} \tag{6.160}$$

The magnitudes of the velocity $\dot{w}_t$ and displacement $w_t$ of the sphere are shown in Fig. 6.19.

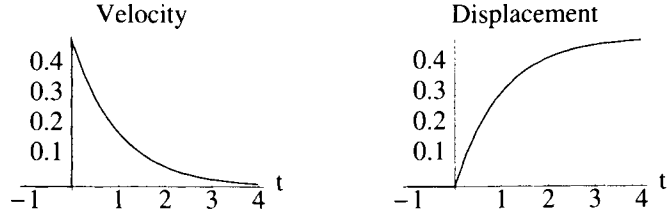


**Figure 6.19:** Velocity and displacement for the sphere, for the case where $\alpha = 1$ and $v$=1.

In this case Eq. (6.159) yields

$$\dot{W}_{mn}(\omega) = \delta_{n1}\delta_{m0}\frac{v}{\alpha - i\omega}. \tag{6.161}$$

The frequency integral in Eq. (6.158) to be evaluated is

$$I(\omega) \equiv \frac{1}{2\pi}\int_{-\infty}^{\infty}\frac{h_1(\omega r/c)}{h_1'(\omega a/c)}\frac{v}{(\alpha - i\omega)}e^{-i\omega t}d\omega \tag{6.162}$$

and Eq. (6.158) is written as

$$p_t(r,\theta,\phi,t) = i\rho_0 c\sum_{n=0}^{\infty}\sum_{m=-n}^{n}Y_n^m(\theta,\phi)I(\omega)\delta_{n1}\delta_{m0}.$$

Using Eq. (6.62)

$$I(\omega) = \frac{va^3}{2\pi r^2}\int_{-\infty}^{\infty}\frac{-e^{ik(r-a)}(i+kr)}{(2i+2ka-i(ka)^2)(\alpha - i\omega)}e^{-i\omega t}d\omega.$$

We can evaluate this integral by contour integration, closing the contour in the lower half plane as shown in Fig. 6.20. The integrand will go to zero on the semicircle as long as $r - a - ct < 0$, so that the quantity

$$e^{i\omega(r-a-ct)/c}$$

is decaying on the semicircle since $\omega$ has a negative imaginary part. For times such that $r - a - ct > 0$ then the contour must be closed in the upper half plane. Since there are

no poles in the upper half plane, then the result of the integration is zero, that is, the sound field has not yet reached the field position $r$ ($r - a > ct$). To communicate this fact to the solution we introduce the Heaviside step function multiplying the solution. Let $H(t)$ be the Heaviside step function defined by

$$\begin{aligned} H(t) &= 0 \quad t < 0 \\ &= 1 \quad t > 0. \end{aligned} \tag{6.163}$$

Thus $H(ct - (r - a))$ with the discontinuity at $r - a - ct = 0$ is correct multiplier.

The zeros of the denominator are at $ka = \pm 1 - i$, or $\omega = (\pm 1 - i)c/a$; and $\omega = -i\alpha$. Thus

$$I(\omega) = \frac{vac^2}{2\pi r^2} \int_{-\infty}^{\infty} \frac{e^{i\omega(r-a-ct)/c}(i + \omega r/c)}{[\omega - (1-i)c/a][\omega - (-1-i)c/a][\omega + i\alpha]} d\omega. \tag{6.164}$$

The contour in the complex plane is shown in Fig. 6.20. The residue theorem states

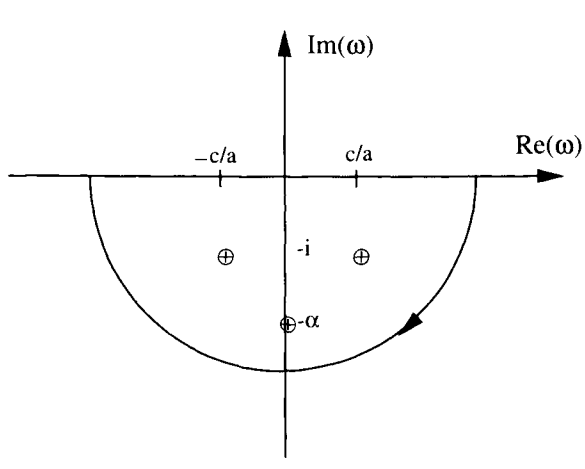


**Figure 6.20:** Complex contour in the $\omega$ plane for the integral in Eq. (6.164).

that

$$I(\omega) = -2\pi i \sum_{j=1}^{3} R_j,$$

where $R_j$ is the residue of the $j$th pole. Thus

$$p_t(r, \theta, \phi, t) = i\rho_0 c \sum_{n=0}^{\infty} \sum_{m=-n}^{n} Y_n^m(\theta, \phi) I(\omega) \delta_{n1} \delta_{m0} = 2\pi \rho_0 c Y_1^0 \sum_{j=1}^{3} R_j.$$

For simplicity we set $\alpha = 0$ so that the motion of the sphere corresponds to an impulse in velocity. After calculation of the residues we find that (the residue from the pole at $\omega = -i0$ being zero)

$$p_t(r, \theta, \phi, t) = \frac{\rho_0 cva}{r} e^{-\beta} (\cos\beta - \sin\beta + \frac{a}{r} \sin\beta) Y_1^0(\theta) H(ct - (r - a)), \tag{6.165}$$

where we have applied the Heaviside step function to the solution and

$$\beta \equiv \frac{ct - (r - a)}{a}.$$

The result, pressure versus $r$, is shown in Fig. 6.21 for four different times at $\theta = 0$. Note that a wake follows the wavefront (sharp edge to the right of the wake). This effect

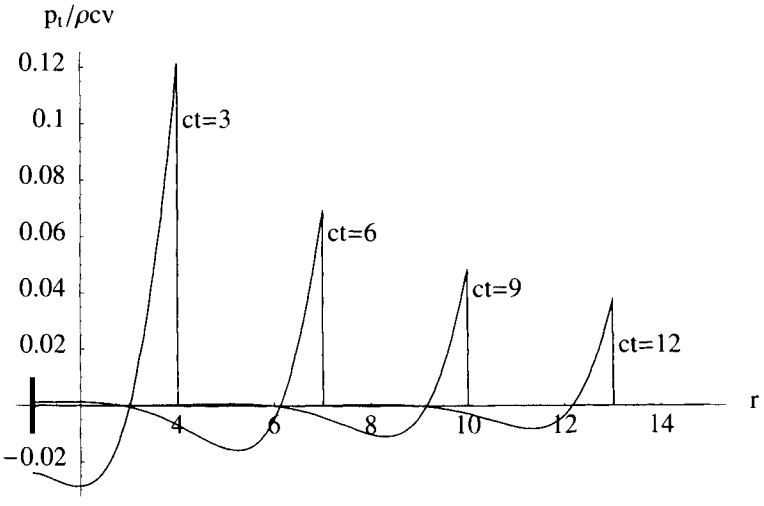


**Figure 6.21:** Normalized pressure from Eq. (6.161) for four different times and $\theta = 0$. For simplicity, $c = a = 1$ and thus $\beta = t - (r - 1)$. The surface of the sphere, shown by the short vertical bar on the left, is at $r = 1$. The impulse occurs on the sphere at $t = 0$.

is due to signals from the various regions of the sphere arriving at the observation point $r$ at different times.

## 6.10 Scattering from Spheres

Although we have not studied scattering from plates or cylinders in this book, we will fill the void with scattering of plane waves from spheres. Important concepts are presented which are needed for practical and theoretical work in acoustics.

### 6.10.1 Formulation

Most scattering problems are formulated for plane wave insonification. The incident field $p_i$ is then represented by a plane wave in the direction $\mathbf{k_i}$ of magnitude $P_0$ as

$$p_i(\mathbf{r}, t) = P_0 e^{i(\mathbf{k_i} \cdot \mathbf{r} - \omega t)} \tag{6.166}$$

where $\mathbf{r}$ is the position vector in a spherical coordinate system, as shown in Fig. 6.22. $\mathbf{k_i}$ or $\mathbf{r}$ may be expanded in terms of its vector components using a spherical or Cartesian

coordinate system. For mathematical simplicity we choose the direction of the plane wave to be along the $z$ axis (which will allow us to use the axisymmetric formulation for the sphere, Section 6.7.9, since the incident field is axisymmetric). This corresponds

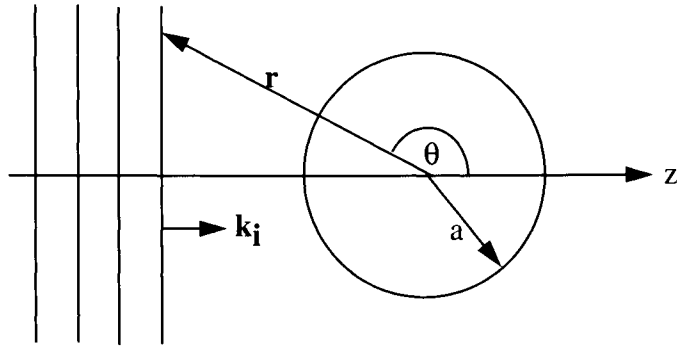


**Figure 6.22:** Direction of the incident plane wave field for scattering from a sphere of radius $a$.

to a point source located on the $z$ axis at $z = -\infty$. Thus $\mathbf{k_i} = k\hat{\mathbf{k}}$ where $k = \omega/c$. We have in the frequency domain then

$$p_i(r, \theta, \phi, \omega) = P_0 e^{ikz} = P_0 e^{ikr\cos\theta} \tag{6.167}$$

which provides the mathematical description of our plane wave in spherical coordinates.

The formulation of the scattering problem involves separating the total pressure field $p_t(r, \theta, \phi, \omega)$ into two parts:

$$p_t = p_s + p_i, \tag{6.168}$$

where $p_i$ is the incident field given above, and $p_s$ is a new quantity called the scattered field. $p_t$ is the total field which corresponds to the pressure which would be measured if one were to carry out a steady state experiment. In Eq. (6.168) $p_i$ remains fixed and independent of the scatterer. In other words, in an experimental sense, the incident field is the field measured without the target (sphere) in place. Then $p_s$ measures the change in the incident field which results when the target is placed in the insonification field. If $p_s$ is zero then the target is completely transparent.

In order to solve the scattering problem mathematically we need to express the *incident* field, Eq. (6.167), on the surface of the sphere; that is, to find an expansion in terms of spherical harmonics which mathematically describes the incident field. We return to our general equation, Eq. (6.21), which provides a solution of the wave equation in terms of spherical harmonics and spherical Bessel functions. Actually, since we know that our source is located at infinity, then the formulation for the interior problem is appropriate as given in Section 6.8. Thus the incident pressure field must be expressible as given in Eq. (6.140):

$$p_i(r, \theta, \omega) = P_0 \sum_{n=0}^{\infty} \sum_{m=-n}^{n} A_{mn}(\omega) j_n(kr) Y_n^m(\theta, \phi), \tag{6.169}$$

which for the axisymmetric case, given arbitrary coefficients $A_n$, is just

$$p_i(r,\theta,\omega) = P_0 e^{ikr\cos\theta} = P_0 \sum_{n=0}^{\infty} A_n j_n(kr) P_n(\cos\theta). \tag{6.170}$$

The relationship between $A_n$ in Eq. (6.170) and $A_{mn}$ in Eq. (6.169) is obtained by multiplication of both sides of Eq. (6.169) by $e^{-im'\phi}$, integrating over $\phi$ and using Eq. (6.53):

$$A_n = A_{0n}\sqrt{\frac{(2n+1)}{4\pi}}.$$

Equation (6.169) expresses the fact that the incident field must be finite at the origin.

To solve for $A_n$ we multiply Eq. (6.170) by $P_n$, integrate over $\theta$ and use the orthogonality, Eq. (6.28), of $P_n$ on the right hand side:

$$\int_0^{\pi} e^{ikr\cos\theta} P_n(\cos\theta)\sin\theta\, d\theta = \frac{2A_n}{2n+1} j_n(kr).$$

Using a change of variables, this equation becomes

$$\int_{-1}^{1} e^{ikr\eta} P_n(\eta) d\eta = \frac{2A_n}{2n+1} j_n(kr). \tag{6.171}$$

If we let $r = 0$ then since $P_n(\eta)$ is orthogonal to 1 (i.e. to $P_0(\eta)$) we find immediately that $A_0 = 1$. To get the other $n$ terms we differentiate with respect to $r$ and evaluate at $r = 0$:

$$\frac{d^n}{dr^n}(e^{ikr\eta}) = (ik\eta)^n e^{ikr\eta}\Big|_{r=0} = (ik\eta)^n.$$

The right hand side of Eq. (6.171) becomes, from Eq. (6.63),

$$\frac{d^n}{dr^n} j_n(kr)\Big|_{r=0} = \frac{d^n}{dr^n}\left(\frac{(kr)^n}{(2n+1)!!}\right) = k^n \frac{n!}{(2n+1)!!}. \tag{6.172}$$

Equating left and right hand sides, and using the relation

$$(2n+1)!! = \frac{(2n+1)!}{2^n n!},$$

we have

$$(ik)^n \int_{-1}^{1} \eta^n P_n(\eta) d\eta = \frac{2A_n}{2n+1} k^n \frac{n!}{(2n+1)!!} = \frac{2A_n}{2n+1} k^n \frac{2^n (n!)^2}{(2n+1)!}.$$

We need the integral relation,

$$\int_{-1}^{1} \eta^n P_n(\eta) d\eta = \frac{2^{n+1}(n!)^2}{(2n+1)!}, \tag{6.173}$$

so our final (and simple) result is,

$$A_n = i^n(2n+1).$$

Inserting this result into Eq. (6.170) we have the important equation

$$e^{ikr\cos\theta} = \sum_{n=0}^{\infty} i^n(2n+1)j_n(kr)P_n(\cos\theta). \tag{6.174}$$

For future reference it is useful to also show the expression for the general case, where the direction of the incident field is given by $(\theta_i, \phi_i)$. In this case the expansion of the incident field is

$$e^{i\vec{\mathbf{k}}_i\cdot\vec{\mathbf{r}}} = 4\pi\sum_{n=0}^{\infty} i^n j_n(kr)\sum_{n=-m}^{m} Y_n^m(\theta,\phi)Y_n^m(\theta_i,\phi_i)^*. \tag{6.175}$$

## 6.10.2 Scattering from a Pressure Release Sphere

Armed with the incident field expanded in spherical harmonics, or Legendre polynomials, we can solve for the pressure field scattered from a sphere of radius $a$ which is pressure release, that is, the *total* pressure on the surface of the sphere must vanish. Thus the boundary condition is

$$p_i(a,\theta) + p_s(a,\theta) = 0. \tag{6.176}$$

Now we must expand the scattered field in terms of spherical harmonics. Since the scattered field represents spherical waves emanating from the surface of the sphere due to scattering from the incident wave, the scattered field is given by outgoing spherical Hankel functions:

$$p_s(r,\theta) = \sum_{n=0}^{\infty} C_n(\omega)h_n^{(1)}(kr)P_n(\cos\theta). \tag{6.177}$$

Inserting Eq. (6.177) and Eq. (6.174) into Eq. (6.176) leads to

$$C_n(\omega) = -P_0(2n+1)i^n\frac{j_n(ka)}{h_n^{(1)}(ka)} \tag{6.178}$$

so that

$$p_s(r,\theta) = -P_0\sum_{n=0}^{\infty}(2n+1)i^n\frac{j_n(ka)}{h_n^{(1)}(ka)}h_n^{(1)}(kr)P_n(\cos\theta). \tag{6.179}$$

The total field (dropping the superscript on the Hankel function) is then

$$p_t(r,\theta) = P_0\sum_{n=0}^{\infty}(2n+1)i^n\left(j_n(kr) - \frac{j_n(ka)}{h_n(ka)}h_n(kr)\right)P_n(\cos\theta). \tag{6.180}$$

In the farfield we use Eq. (6.68) to obtain the scattered field from Eq. (6.179):

$$\lim_{r\to\infty} p_s(r,\theta) = iP_0\frac{e^{ikr}}{kr}\sum_{n=0}^{\infty}(2n+1)\frac{j_n(ka)}{h_n(ka)}P_n(\cos\theta). \tag{6.181}$$

Note it does not make sense to try to write the total field in the farfield since the incident field has a singularity there. At low frequencies using Eq. (6.63) and Eq. (6.64),

$$\lim_{ka\to 0} \frac{j_n(ka)}{h_n(ka)} = ika,$$

so that the scattered pressure becomes

$$p_s(r,\theta) \approx -P_0 a \frac{e^{ikr}}{r}. \tag{6.182}$$

### 6.10.3 Scattering from a Rigid Sphere

For a rigid sphere the radial velocity vanishes on the surface of a sphere at $r = a$. This is the total radial velocity (including incident and scattered). The boundary condition is then

$$\dot{w}_t(a,\theta) = \dot{w}_i(a,\theta) + \dot{w}_s(a,\theta) = 0. \tag{6.183}$$

By Euler's equation Eq. (6.183) can be written as

$$\frac{\partial}{\partial r}\Big(p_i(r,\theta) + p_s(r,\theta)\Big)\Big|_{r=a} = 0. \tag{6.184}$$

Again, as in Eq. (6.177), the scattered field is expanded in outgoing waves:

$$p_s(r,\theta) = \sum_{n=0}^{\infty} C_n(\omega) h_n^{(1)}(kr) P_n(\cos\theta),$$

with the incident field given by Eq. (6.174).

$$p_i(r,\theta) = P_0 \sum_{n=0}^{\infty} i^n (2n+1) j_n(kr) P_n(\cos\theta).$$

Using these expressions in Eq. (6.184) yields,

$$C_n = -P_0(2n+1) i^n \frac{j_n'(ka)}{h_n'(ka)}$$

so that

$$p_s(r,\theta) = -P_0 \sum_{n=0}^{\infty} (2n+1) i^n \frac{j_n'(ka)}{h_n'(ka)} h_n(kr) P_n(\cos\theta). \tag{6.185}$$

The total field is then

$$p_t(r,\theta) = P_0 \sum_{n=0}^{\infty} (2n+1) i^n \left( j_n(kr) - \frac{j_n'(ka)}{h_n'(ka)} h_n(kr) \right) P_n(\cos\theta). \tag{6.186}$$

The farfield scattered pressure, using Eq. (6.68), is

$$\lim_{r\to\infty} p_s(r,\theta) = iP_0 \frac{e^{ikr}}{kr} \sum_{n=0}^{\infty} (2n+1) \frac{j_n'(ka)}{h_n'(ka)} P_n(\cos\theta). \tag{6.187}$$

We now consider the farfield pressure at low frequencies. We will keep the first two terms of the series in Eq. (6.187). Thus,

$$p_s \approx iP_0 \frac{e^{ikr}}{kr}\left(\frac{j_0'(ka)}{h_0'(ka)} + \frac{3j_1'(ka)}{h_1'(ka)}\cos\theta\right) \approx P_0 \frac{e^{ikr}}{r}\frac{k^2a^3}{3}\left(\frac{3}{2}\cos\theta - 1\right). \tag{6.188}$$

Now we see why we took two terms of the series. Both the $n = 0$ and the $n = 1$ terms are of the same order in $ka$. In the low frequency limit the scattered field from a rigid sphere consists of a monopole term and dipole term.

Returning to the general solution, Eq. (6.185), we define the normalized farfield scattered pressure $\bar{p}_s$ by

$$\bar{p}_s(\theta) \equiv \lim_{r\to\infty} p_s(r,\theta)\frac{r}{P_0 a}e^{-ikr}, \tag{6.189}$$

with $\lim_{r\to\infty} p_s(r,\theta)$ given by Eq. (6.187). This leads to

$$\bar{p}_s(\theta) \equiv i\sum_{n=0}^{\infty}(2n+1)\frac{j_n'(ka)}{(ka)h_n'(ka)}P_n(\cos\theta). \tag{6.190}$$

This normalization provides a dimensionless quantity with $e^{ikr}/r$ removed. Some results for $\bar{p}_s(\theta)$ are plotted in Fig. 6.23. In the figure the plane wave is incident from the left. The large peaks along the $z$ axis for $ka = 10$ and 20 are due to the shadowing effect of the sphere which causes the *total* pressure to diminish behind it. At low frequencies the backscattering ($\theta = \pi$) dominates over the forward scatter. For high frequencies the scattering becomes omnidirectional reaching a value of 0.5 for all angles except forward scatter ($\theta = 0$).

The differential cross-section $d\sigma/d\Omega$ is defined as the square of the magnitude of the directivity function of the farfield pressure normalized to the incident pressure:

$$d\sigma/d\Omega \equiv |D(\theta,\phi)/P_0|^2 \tag{6.191}$$

where $D$ was defined, as in Eq. (2.85) on page 39 (given by the farfield pressure with the term $e^{ikr}/r$ factored out), as

$$\lim_{r\to\infty} p_s(r,\theta,\phi) = \frac{e^{ikr}}{r}D(\theta,\phi).$$

Thus for the farfield scattered pressure field, we remove the term $e^{ikr}/r$ to arrive at the differential cross-section:

$$d\sigma/d\Omega = \lim_{r\to\infty}\left|\frac{r}{P_0 e^{ikr}}p_s(r,\theta,\phi)\right|^2. \tag{6.192}$$

Another definition of use in underwater acoustics is the target strength, TS. It is defined by

$$\mathrm{TS} = 10\log_{10}\left(\frac{d\sigma/d\Omega}{r_{\mathrm{ref}}^2}\right), \tag{6.193}$$

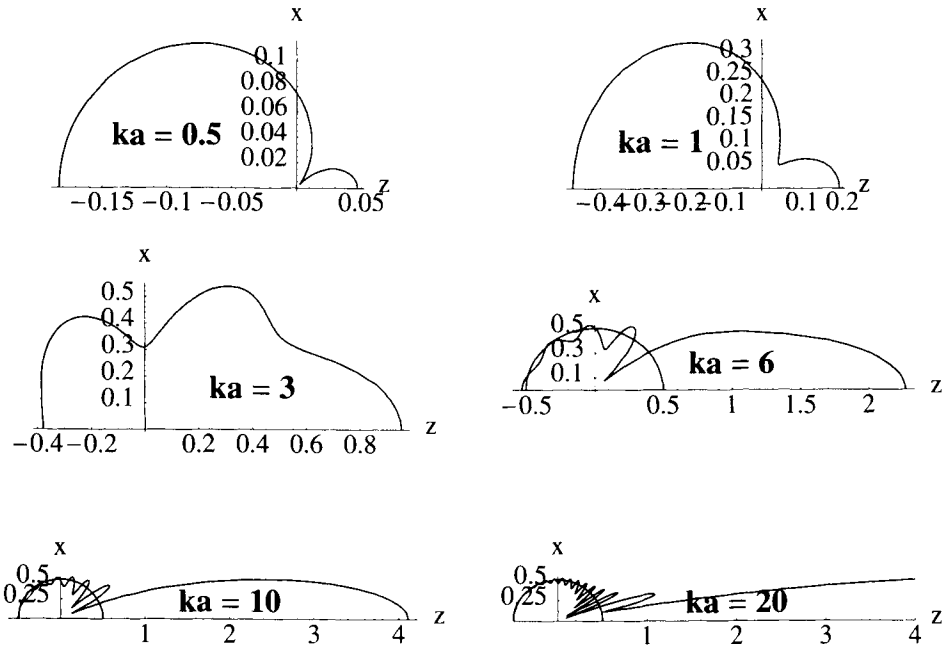


**Figure 6.23:** The magnitude of the normalized scattered farfield pressure for a rigid sphere, using Eq. (6.190), for various $ka$. The plane wave is incident from the left. Note that as $ka \to \infty$ that $\bar{p}_s(\theta) = 0.5$ except at $\theta = 0$ (forward scatter) where it is infinite.

where $r_{\text{ref}}$ is a reference distance taken as 1 m. (Older definitions used a one yard reference.) Comparison of Eq. (6.192) with Eq. (6.189) indicates that

$$d\sigma/d\Omega = \left|a\bar{p}_s(\theta,\phi)\right|^2. \tag{6.194}$$

At low frequencies, from Eq. (6.188), we see that

$$\frac{1}{a}\sqrt{\frac{d\sigma}{d\Omega}} = \bar{p}_s = \frac{k^2a^2}{3}\left|\frac{3}{2}\cos\theta - 1\right|. \tag{6.195}$$

Note that the quantity plotted in Fig. 6.23, $\bar{p}_s$, is the square root of the differential cross-section divided by the radius. Thus at high frequencies since $\bar{p}_s$ approaches 1/2, so the target strength approaches

$$\text{TS} = 10\log_{10}(a/2)^2. \tag{6.196}$$

### 6.10.4 Scattering from an Elastic Body

There is a very powerful formulation for the solution to the scattering from bodies (not necessarily spherical) which are elastic. We present this formulation in this section for the spherical body. This technique essentially turns the scattering problem into a radiation problem by formulating a "blocked" pressure. We now describe this formulation.[10]

As usual the total pressure is made up of the incident and scattered pressure,

$$p_t = p_i + p_{se}, \tag{6.197}$$

where we have added the $e$ subscript on the scattered term to indicate an elastic body. As always the total normal velocity at the body surface is given by Euler's equation,

$$\dot{w}_t = \frac{1}{i\rho_0 ck}\frac{\partial p_t}{\partial r} = \frac{1}{i\rho_0 ck}\left(\frac{\partial p_i}{\partial r} + \frac{\partial p_{se}}{\partial r}\right). \tag{6.198}$$

At this point we break the scattered field into two components, the first being the field produced if the sphere were rigid, $p_{s\infty}$ (the $\infty$ subscript indicates infinite impedance), and the second, $p_r$; what is left over as a result of elasticity. Thus we write the scattered pressure as

$$p_{se} = p_{s\infty} + p_r, \tag{6.199}$$

where $p_{s\infty}$ does not depend on the sphere's elasticity, and $p_r$ now contains the elastic dependencies. With these definitions, Eq. (6.198) becomes

$$\dot{w}_t = \frac{1}{i\rho_0 ck}\Big(\underbrace{\frac{\partial p_i}{\partial r} + \frac{\partial p_{s\infty}}{\partial r}}_{=0} + \frac{\partial p_r}{\partial r}\Big), \tag{6.200}$$

where the first two terms, evaluated at $r = a$, are zero due to Eq. (6.184) (definition of a rigid body). These terms correspond to the first two terms (at $r = a$) of

$$p_t = \underbrace{p_i + p_{s\infty}}_{\text{rigid}} + p_r = p_b + p_r, \tag{6.201}$$

where $p_b \equiv p_i + p_{s\infty}$ is defined as the *blocked pressure*. Thus the total velocity at the surface of the sphere depends only on $p_r$. That is,

$$\dot{w}_t(a,\theta,\phi) = \frac{1}{i\rho_0 ck}\frac{\partial p_r(a,\theta\phi)}{\partial r}. \tag{6.202}$$

Now we ask, "to what problem do these last two equations provide a solution?" The key is in the fact that in Eq. (6.202) only $p_r$ contributes to the total velocity at the surface of the sphere, and this velocity is independent of the gradient of the blocked pressure. In view of Eq. (6.106), once the radial surface velocity is specified (through Eq. (6.202)), then the pressure from the surface to the farfield is uniquely determined, and that pressure must then be $p_r(r,\theta,\phi)$. But at the same time, in order to satisfy Eq. (6.201) which represents the total force per unit area on the surface of the sphere,

[10] Junger and Feit, *Sound, Structures, and their Interactions*, Chapter 11.

we must think of $p_b$ not as an acoustic pressure, but as an internal force generated at the boundary, like a layer of infinitesimally small shakers driving the elastic sphere from the inside with the prescribed force distribution $p_b$. These shakers excite the elastic sphere causing it to radiate a pressure field $p_r$.

To sum up the formulation for scattering from an elastic body,

(1) Solve the rigid body problem, calculating the total pressure at the surface (the blocked pressure $p_b$) and the scattered pressure over all space $p_{s\infty}(r, \theta, \phi)$.

(2) Solve the radiation problem with $-p_b$ the forcing function at the surface of the elastic body, to obtain the radiated pressure $p_r(r, \theta, \phi)$.

(3) The solution to the scattering problem $p_{se}$ is now the sum $p_{s\infty} + p_r$ and the total field is just $p_t = p_i + p_{s\infty} + p_r$.

# Problems

**6.1** Find the general expression for the pressure inside a sphere of radius $a$ if the pressure on the surface is given as $p(a, \theta, \phi)$.

**6.2** Find the pressure between concentric spheres of radii $b > a$ if the pressure is zero on the inner sphere and $p(b, \theta, \phi)$ on the outer.

**6.3** Small spherical caps (small enough to be considered point sources) with area $A$ at the North and South poles of a sphere of radius $a$ vibrate 180 degrees out of phase while the rest of the sphere is rigid. Calculate the radiation pattern and the total average power radiated if $ka << 1$.

**6.4** A sphere of radius $a$ vibrates with normal velocity $V \sin^2\theta e^{-i\omega t}$. Calculate the total average power radiated. Hint: $\sin^2\theta = \frac{2}{3}[P_0(\cos\theta) - P_2(\cos\theta)]$.

**6.5** Find the normal velocity distribution on a sphere of radius $a$ which would produce a farfield pressure $p_0(\theta, \phi)$.

**6.6** A small spherical cap with angular width $\theta_0$ on an otherwise rigid sphere consists of two halves which vibrate 180 degrees out of phase. Thus,

$$\begin{aligned} \dot{w}(a, \theta, \phi) &= +V \quad 0 \le \phi < \pi, \quad \theta < \theta_0 \\ &= -V \quad \pi \le \phi < 2\pi, \quad \theta < \theta_0. \end{aligned}$$

Obtain approximate expressions for the farfield radiation pattern and the total average power radiated assuming $ka << 1$, where $a$ is the radius of the sphere.

**6.7** A rigid sphere is oscillating with radial velocity $\dot{w}(\theta) = \dot{w}_0 \cos\theta$. Compute the farfield pressure valid for all frequencies. What is the low frequency limit?

**6.8** Use separation of variables, Eq. (6.7), to derive the 4 differential equations, Eqs (6.8 6.11).

**6.9** Demonstrate by integration that $Y_3^2(\theta, \phi)$ and $Y_3^3(\theta, \phi)$ are orthonormal.

**6.10** Demonstrate by integration that $P_3^1(\cos\theta)$ and $P_2^1(\cos\theta)$ are orthogonal.

**6.11** The pressure from a longitudinal quadrupole oriented along the $z$ axis is given by

$$p = -i\rho_0 ckQzz \frac{\partial^2}{\partial z'^2} G(\mathbf{r}|\mathbf{r}')\Big|_{r'=0}.$$

Perform the indicated differentiation and show that the result can be written as proportional to the weighted sum of two spherical harmonics, $Y_2^0$ and $Y_0^0$, that is, $p = A_2(r)Y_2^0 + A_0(r)Y_0^0$. Determine the weighting factors, $A_2$ and $A_0$.

**6.12** Calculate the power radiated from the sphere with the vibrating cap, in Section 6.7.10 using Eq. (6.134).

**6.13** Compute the farfield pressure from Eq. (6.134). Compute the farfield pressure at very low frequencies. Do you need to keep the $n = 1$ term in comparison with the $n = 0$ term?

**6.14** Compute $\dot{w}$, $\dot{u}$, $e_{av}$, $I_r$, $I_\theta$ and the total power radiated, $\Pi$, for the dipole in Section 6.5.2.

**6.15** For an interior problem Eq. (6.111) also provides the power transmitted to the inside. Using Eq. (6.140) prove that the power transmitted to the interior of a vibrating sphere of radius $a$ is identically zero.

**6.16** Compute the differential cross-section and the target strength for the scattering of a plane wave from a pressure release sphere.

**6.17** Compute the scattering from a sphere of radius $a$ filled with fluid of density and sound speed, $\rho_1$, $c_1$, and surrounded by fluid of density $\rho_0$ and sound speed, $c_0$. The boundary conditions at the surface of the sphere are continuity of radial velocity and pressure (no surface tension) between the two fluids. Show that your answer matches that of the pressure release and rigid spheres when $c_1 \to 0$ and $c_1 \to \infty$, respectively.

**6.18** A rigid sphere of radius $a$ with center at the origin is oscillating in the $z$ direction so that its radial surface velocity is given by

$$\dot{w}(a, \theta) = v\cos\theta.$$

(a) Find the solution for the radiated pressure which is valid everywhere outside the sphere.

(b) Write this solution in terms of spherical harmonics.

(c) We change the direction of oscillation so that now the sphere is oscillating in the $y$ direction. The radial velocity is now given by

$$\dot{w}(a, \theta) = v\sin\theta\sin\phi.$$

Using the nonaxisymmetric version of the exterior problem, again find the pressure outside of the sphere.

(d) Note that the radius vector to the field point (where we measure the pressure) is given by the spherical coordinates, $\theta$ and $\phi$, and that the projection of that radius vector onto the $y$ axis is simply $r\sin\theta\sin\phi$. If we define the angle between the radius vector and the $y$ axis as $\gamma$, then we notice that the motion of the sphere could be described simply in terms of this angle as

$$\dot{w}(a,\theta) = v\cos\gamma.$$

Equating the projections of the radius vector onto the $y$ axis yields

$$\cos\gamma = \sin\theta\sin\phi.$$

Use this fact to show that the two solutions which you derived in parts (1) and (3) are identical (interpreting the angle $\gamma$ as the polar angle, and the $y$ axis the polar axis).

**6.19** A small piston set in a rigid sphere (see Fig. 6.15) vibrates with a constant radial velocity, (independent of $\phi$), $\dot{w}(a,\theta)$ given by

$$\begin{aligned}\dot{w}(a,\theta) &= \dot{W}, \qquad 0 \le \theta \le \alpha \\ &= 0, \qquad \alpha < \theta \le \pi.\end{aligned}$$

(a) Solve for the pressure field, $p(r,\theta)$, **inside** the sphere. In your solution you can assume that $\alpha$ is small enough so that one can replace $P_n(\cos\alpha)$ with unity.

(b) Keeping the $n = 0$ and $n = 1$ terms what is the low frequency approximation to the pressure in the interior?

(c) The motion of the piston generates a force equal to its area times the pressure generated at its inner surface. This defines a mechanical impedance given by $F/\dot{W}$. As $k \to 0$ show that this impedance is spring like. What is the equivalent stiffness of the air spring given by this impedance? Keep your answer in terms of $\alpha$ (not in terms of volume flow).

**6.20** Write down (no algebra required!) the value of the sum,

$$\sum_{n=m}^{\infty} \frac{2n+1}{2}\frac{(n-m)!}{(n+m)!}P_n^m(x)P_n^m(y).$$

What is the significance of this result?